2012). Therefore, it is widely recognized that TGF-β plays important roles in the regulation of bone remodeling by connecting bone resorption and bone formation (Tang et al., 2009). Regarding the intracellular signaling of TGF-β, these effects are exerted mainly through the canonical pathway dependent upon Smads such as Smad2 and Smad3 (ten Dijke and Hill, 2004). On the other hand, TGF-β reportedly functions via Smad-independent, non-canonical pathways such as mitogen-activated protein (MAP) kinases (Moustakas and Heldin, 2005). In our previous studies (Kanno et al., 2005; Tokuda et al., 2003), we have demonstrated that TGF-β stimulates VEGF synthesis in osteoblast-like MC3T3-E1 cells and that this synthesis is positively regulated via p44/p42 MAP kinase, p38 MAP kinase and stress-activated protein kinase/c-*Jun* N-terminal kinase (SAPK/JNK). Therefore, the TGF-β signaling involved in VEGF synthesis in osteoblasts is complicated, and the exact mechanism remains to be clarified.

Rac is a member of the Rho family of small GTPases (Takai et al., 2001). Rac is generally known to be inactive when bound to GDP and subsequently activated upon the exchange of GDP to GTP, leading to downstream signaling. Rac is also well recognized to be ubiquitously expressed in numerous types of cells and functions to regulate actin cytoskeletal reorganization. As for osteoblasts, it has recently been reported that Rac is essential for cell adhesion, spreading and proliferation (Jung et al., 2011). However, the precise mechanism underlying the effects of Rac on osteoblasts has not yet been clarified.

In the present study, we investigated the role of Rac in the TGF-β-stimulated VEGF synthesis in osteoblast-like MC3T3-E1 cells. We herein show that Rac negatively regulates the TGF-β-stimulated VEGF synthesis via the inhibition of p38 MAP kinase in these cells.

2. Materials and methods

2.1. Materials

TGF-β and the mouse VEGF enzyme-linked immunosorbent assay (ELISA) kit were obtained from R&D Systems, Inc. (Minneapolis, MN). A Rac1 Activation Assay kit was obtained from EMD Millipore Corp. (Temecula, CA). NSC23766 was obtained from Tocris Bioscience (Bristol, UK). SIS3 was obtained from Calbiochem-Novabiochem Co. (La Jolla, CA). Phospho-specific Smad2 antibodies, phospho-specific Smad3 antibodies, Smad2/3 antibodies, phospho-specific p44/p42 MAP kinase antibodies, p44/p42 MAP kinase antibodies, phospho-specific SAPK/JNK antibodies, SAPK/JNK antibodies, phospho-specific p38 MAP kinase antibodies and p38 MAP kinase antibodies were obtained from Cell Signaling Technology, Inc. (Beverly, MA). An ECL Western blotting detection system was obtained from GE Healthcare UK Ltd. (Buckinghamshire, UK). Control siRNA (Silencer Negative Control no.1 siRNA) was obtained from Ambion (Austin, TX). Rac-siRNA (3_RNAI) was obtained from Invitrogen Corp. (Carlsbad, CA). Other materials and chemicals were obtained from commercial sources.

2.2. Cell culture

Cloned osteoblast-like MC3T3-E1 cells derived from newborn mouse calvaria (Sudo et al., 1983) were maintained as previously described (Kozawa et al., 1992). Briefly, the cells were cultured in α-minimum essential medium (α-MEM) containing 10% fetal bovine serum (FBS) at 37 °C in a humidified atmosphere of 5% CO_2/95% air. The cells were seeded into 35-mm diameter dishes (5×10^4 cells/dish) or 90-mm diameter dishes (2×10^5 cells/dish) in α-MEM containing 10% FBS. After 5 days, the medium was exchanged for α-MEM containing 0.3% FBS. The cells were used for the experiments after 48 h.

2.3. Assay for VEGF

The cultured cells were pretreated with various doses of NSC23766, 7 μM of SIS3 or vehicle for 60 min, and then stimulated by TGF-β or vehicle in 1 ml of α-MEM containing 0.3% FBS for 48 h. The conditioned medium was collected at the end of incubation, and the VEGF concentration was then measured using the VEGF ELISA kit according to the manufacturer's protocol.

2.4. Real-time RT-PCR

The cultured cells were pretreated with various doses of NSC23766 for 60 min, and then stimulated by TGF-β or vehicle in α-MEM containing 0.3% FBS for 12 h. Total RNA was isolated and transcribed into complementary DNA using TRIzol reagent (Invitrogen Corp.) and the Omniscript Reverse Transcriptase kit (QIAGEN, Inc., Valencia, CA), respectively. Real-time RT-PCR was performed using a Light Cycler system in capillaries and the Fast Start DNA Master SYBR Green I provided with the kit (Roche Diagnostics, Basel, Switzerland). Sense and antisense primers for mouse VEGF mRNA and Glyceraldehyde-3-phosphate dehydrogenase (GAPDH) mRNA were purchased from Takara Bio, Inc. (Tokyo, Japan) (primer set ID: MA039013). The amplified products were determined using a melting curve analysis and agarose electrophoresis. The VEGF mRNA levels were normalized to those of GAPDH mRNA.

2.5. siRNA transfection

In order to knockdown Rac in MC3T3-E1 cells, the cells were transfected with negative control siRNA or Rac-siRNA utilizing siLentFect according to the manufacturer's protocol. In brief, the cells were seeded into 35-mm diameter dishes (1×10^5 cells/dish) in α-MEM containing 10% FBS and subcultured for 48 h. The cells were then incubated at 37 °C with 50 or 70 nM siRNA-siLentFect complexes. After 24 h, the medium was exchanged to α-MEM containing 0.3% FBS. Then, the cells were stimulated by TGF-β in α-MEM containing 0.3% FBS for the indicated periods.

2.6. Western blot analysis

The cultured cells were pretreated with various doses of NSC23766 for 60 min, and then stimulated by TGF-β or vehicle in α-MEM containing 0.3% FBS for the indicated periods. The cells were washed twice with phosphate-buffered saline and then lysed, homogenized and sonicated in a lysis buffer containing 62.5 mM Tris/HCl, pH 6.8, 2% sodium dodecyl sulfate (SDS), 50 mM dithiothreitol and 10% glycerol. SDS-polyacrylamide gel electrophoresis (PAGE) was performed by the method of Laemmli (Laemmli, 1970) in 10% polyacrylamide gels. The proteins were fractionated and transferred onto Immun-Blot polyvinyl difluoride (PVDF) Membranes (Bio-Rad, Hercules, CA). The membranes were blocked with 5% fat-free dry milk in Tris-buffered saline-Tween (TBS-T; 20 mM Tris/HCl, pH 7.6, 137 mM NaCl, 0.1% Tween-20) for 2 h before incubation with the primary antibodies. A Western blot analysis was performed as previously described (Kato et al., 1996) using phospho-specific Smad2 antibodies, phospho-specific Smad3 antibodies, Smad2/3 antibodies, phospho-specific p44/p42 MAP kinase antibodies, p44/p42 MAP kinase antibodies, phospho-specific SAPK/JNK antibodies, SAPK/JNK antibodies, phospho-specific p38 MAP kinase antibodies or p38 MAP kinase antibodies as primary antibodies, with peroxidase-labeled antibodies raised in goat against rabbit IgG used as secondary antibodies. The primary and secondary antibodies were diluted at 1:1000 with 5% fat-free dry milk in TBS-T. The peroxidase activity on the PVDF sheet was visualized on an X-ray film by means of the ECL Western blotting detection system.

2.7. Measurement of Rac activity

The Rac activity was determined using the Rac1 Activation Assay kit according to the manufacturer's protocol. In brief, the cultured cells were stimulated by TGF-β for the indicated periods and washed twice with TBS. The cells were then detached from the plates by scraping and centrifuged at 2000 × *g* at 4 °C for 1 min. The supernatant was discarded, and the cells were dissolved in the lysis buffer provided with the assay kit. GTP-bound Rac was immunoprecipitated as described in the manufacturer's protocol. The immunoprecipitated GTP-bound Rac and pre-immunoprecipitated lysates (Rac) were subjected to SDS-PAGE with a subsequent Western blot analysis using the corresponding antibodies provided with the assay kit.

2.8. Determination

The absorbance of the enzyme immunoassay samples was measured at 450 nm with the EL 340 Bio Kinetic Reader (Bio-Tek Instruments, Inc., Winooski, VT). A densitometric analysis was performed using a scanner and image analysis software package (image J version 1.45). The phosphorylated protein levels were calculated as follows: the background-subtracted signal intensity of each phosphorylation signal was respectively normalized to the total protein signal and plotted as the fold increase in comparison with that of the control cells treated without stimulation.

2.9. Statistical analysis

The data were analyzed using an ANOVA followed by the Bonferroni method for multiple comparisons between pairs, and a *P* value of <0.05 was considered to be statistically significant. All data are presented as the mean ± standard error of the mean (SEM) of triplicate determinations from three independent cell preparations.

3. Results

3.1. Effect of TGF-β on the Rac activation in MC3T3-E1 cells

We first investigated whether TGF-β induces the activation of Rac in osteoblast-like MC3T3-E1 cells. Rac is known to be a component of the Rho family of small GTPase and exists in two conformational states, a GTP-bound active form and a GDP-bound inactive form (Etienne-Manneville and Hall, 2002). Guanine nucleotide exchange factors (GEFs) promote the exchange of GDP for GTP to generate the activation of Rac (Takai et al., 2001). Therefore, we examined the effect of TGF-β on the levels of GTP-bound Rac in MC3T3-E1 cells. TGF-β time-dependently increased the GTP-bound Rac levels in these cells (Fig. 1). The maximum increase in GTP-bound Rac was observed from 20 to 30 min after TGF-β-stimulation, and the levels decreased thereafter.

3.2. Effect of NSC23766 on the TGF-β-stimulated VEGF release in MC3T3-E1 cells

In order to investigate whether Rac is involved in the VEGF synthesis induced by TGF-β in osteoblast-like MC3T3-E1 cells, we examined the effect of NSC23766, a selective inhibitor of Rac-GEF interaction (Gao et al., 2004), on the TGF-β-stimulated VEGF release in MC3T3-E1 cells. NSC23766, which alone hardly affected the release of VEGF, significantly amplified the TGF-β-stimulated VEGF release (Fig. 2). The maximum effect of NSC23766 on the VEGF release was observed at 200 μM, thus resulting in an approximately 90% enhancement in the TGF-β-effect.

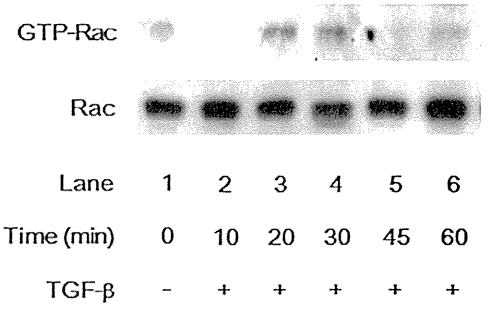

Fig. 1. Effect of TGF-β on the Rac activation in MC3T3-E1 cells. The cultured cells were stimulated by 5 ng/ml of TGF-β for the indicated periods. Samples were prepared as described in Section 2, and GTP-bound Rac was immunoprecipitated using the Rac1 Activation Assay kit. The immunoprecipitated GTP-bound Rac and pre-immunoprecipitated lysates (Rac) were subjected to SDS-PAGE with a subsequent Western blot analysis using antibodies against Rac.

3.3. Effect of NSC23766 on the TGF-β-stimulated VEGF release in the Rac-knock down MC3T3-E1 cells

Additionally, in order to elucidate the involvement of Rac in the TGF-β-stimulated VEGF synthesis, we established Rac-knock down MC3T3-E1 cells transfected with Rac-siRNA and examined the TGF-β-effect on VEGF release in comparison with that seen in negative control siRNA-transfected cells. TGF-β-stimulated VEGF release was significantly enhanced in the Rac-knock down cells (Table 1).

3.4. Effect of NSC23766 on the TGF-β-induced expression of VEGF mRNA in MC3T3-E1 cells

In order to elucidate whether the enhancement of TGF-β-stimulated VEGF release induced by NSC23766 is mediated via

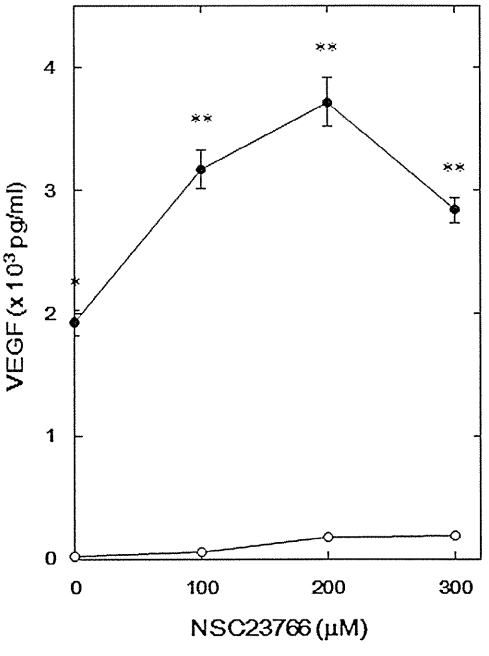

Fig. 2. Effect of NSC23766 on the TGF-β-stimulated VEGF release in MC3T3-E1 cells. The cultured cells were pretreated with various doses of NSC23766 for 60 min, and then stimulated by 3 ng/ml of TGF-β (●) or vehicle (○) for 48 h. The VEGF concentrations in the culture medium were determined using ELISA. Each value represents the mean ± SEM of triplicate determinations from three independent cell preparations. *$P < 0.05$, compared with the value of the control. **$P < 0.05$, compared with the value of TGF-β alone.

Table 1
Effect of TGF-β on VEGF release in the Rac-knocked down MC3T3-E1 cells.

siRNA	TGF-β	VEGF (pg/ml)
Neg	–	57 ± 7
Neg	+	2806 ± 35*
Rac	–	434 ± 18
Rac	+	3533 ± 105**

The cultured cells were transfected with 70 nM negative control siRNA (Neg) or 70 nM Rac-siRNA (Rac) using the siLentFect. After transfection, the cells were stimulated by 3 ng/ml of TGF-β or vehicle for 48 h. The VEGF concentrations of the medium were determined using ELISA. Each value represents the mean ± SEM of triplicate independent determinations. The VEGF level was corrected for the total protein level.
* $P < 0.05$, compared with the value of vehicle with negative control siRNA transfection.
** $P < 0.05$, compared with the value of TGF-β with negative control siRNA transfection.

transcriptional events, we examined the effect of NSC23766 on the TGF-β-induced VEGF mRNA expression using real-time RT-PCR. NSC23766 markedly increased the TGF-β-induced VEGF mRNA expression levels in a dose-dependent manner (Fig. 3).

3.5. Effect of SIS3 on the TGF-β-stimulated VEGF release in MC3T3-E1 cells

As for the intracellular signaling of TGF-β, the effects of TGF-β are mediated mainly through the Smad-dependent pathway (Miyazawa et al., 2002). Hence, in order to investigate whether the Smad-dependent pathway is implicated in the TGF-β-stimulated VEGF synthesis, we examined the effect of SIS3, a specific inhibitor of TGF-β-dependent Smad3 phosphorylation (Jinnin et al., 2006),

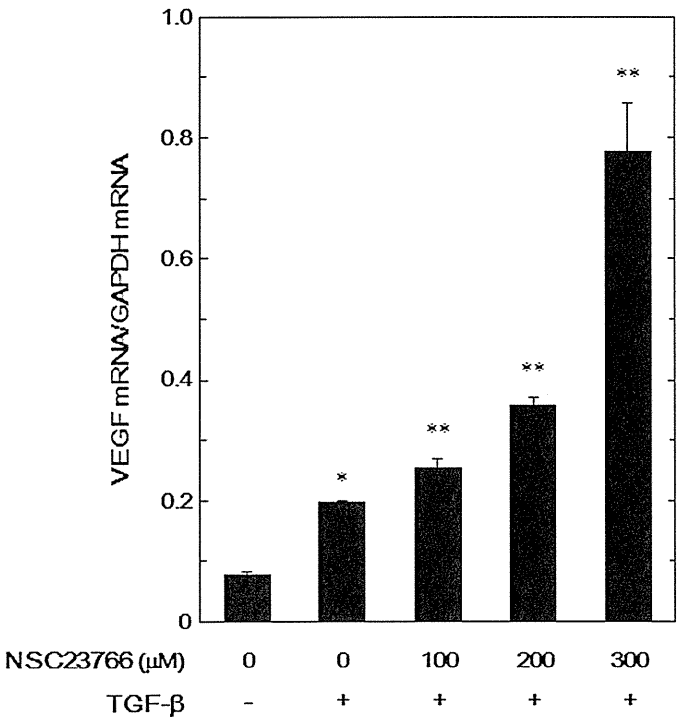

Fig. 3. Effect of NSC23766 on the TGF-β-induced expression of VEGF mRNA in MC3T3-E1 cells. The cultured cells were pretreated with various doses of NSC23766 for 60 min, and then stimulated by 3 ng/ml of TGF-β or vehicle for 12 h. The respective total RNA was then isolated and quantified using real-time RT-PCR. Each value represents the mean ± SEM of triplicate determinations from three independent cell preparations. *$P < 0.05$, compared with the value of the control. **$P < 0.05$, compared with the value of TGF-β alone.

Table 2
Effect of SIS3 on the TGF-β-stimulated VEGF release in MC3T3-E1 cells.

SIS3 (7 μM)	TGF-β	VEGF (pg/ml)
–	–	21 ± 1
–	+	7175 ± 396*
+	–	516 ± 2
+	+	1804 ± 60**

The cultured cells were pretreated with 7 μM of SIS3 or vehicle for 60 min, and then stimulated 5 ng/ml of TGF-β or vehicle for 48 h. The VEGF concentrations of the medium were determined using ELISA. Each value represents the mean ± SEM of triplicate independent determinations.
* $P < 0.05$, compared with the value of the control.
** $P < 0.05$, compared with the value of TGF-β alone.

on the VEGF release stimulated by TGF-β. SIS3 significantly reduced the TGF-β-stimulated VEGF release in these cells (Table 2).

3.6. Effect of NSC23766 on the TGF-β-induced phosphorylation of Smad2 and Smad3 in MC3T3-E1 cells

In order to further investigate whether the effect of Rac on the TGF-β-stimulated VEGF synthesis is related to Smad2 and/or Smad3 activation, we examined the effects of NSC23766 on the TGF-β-induced phosphorylation of Smad2 or Smad3 in MC3T3-E1 cells. However, NSC23766 failed to affect the phosphorylation of Smad2 or Smad3 induced by TGF-β in these cells (Fig. 4).

3.7. Effects of NSC23766 on the TGF-β-induced phosphorylation of p44/p42 MAP kinase, p38 MAP kinase and SAPK/JNK in MC3T3-E1 cells

It is firmly established that TGF-β exerts its effects on a variety of biological cell functions via the Smad-independent pathway in addition to the Smad-dependent pathway (Moustakas and Heldin, 2005). We have previously reported that TGF-β stimulates VEGF synthesis via p44/p42 MAP kinase, p38 MAP kinase and SAPK/JNK in osteoblast-like MC3T3-E1 cells (Kanno et al., 2005; Tokuda et al., 2003). Therefore, we next examined the effects of NSC23766 on the TGF-β-induced phosphorylation of p44/p42 MAP kinase, p38 MAP kinase and SAPK/JNK in MC3T3-E1 cells. NSC23766, hardly affected the TGF-β-induced phosphorylation of p44/p42 MAP kinase (Fig. 5) or SAPK/JNK (data not shown). In contrast, NSC23766 (300 μM) significantly strengthened the TGF-β-induced phosphorylation of p38 MAP kinase (Fig. 6).

3.8. Effect of TGF-β on the phosphorylation of p38 MAP kinase in the Rac-knock down MC3T3-E1 cells

In order to further clarify the relationship between Rac and p38 MAP kinase in the process of TGF-β-induced intracellular signaling in osteoblast-like MC3T3-E1 cells, we examined the effect of TGF-β on the phosphorylation of p38 MAP kinase in the Rac-knock down MC3T3-E1 cells with Rac-siRNA. Consequently, the TGF-β-induced phosphorylation of p38 MAP kinase was markedly enhanced in the Rac-knock down cells compared with that seen in the negative control siRNA-transfected cells (Fig. 7).

4. Discussion

In the present study, we investigated the involvement of Rac, a member of the Rho family of small GTPases, in the TGF-β-stimulated VEGF synthesis in osteoblast-like MC3T3-E1 cells and the underlying mechanism. We demonstrated that TGF-β increased the GTP-bound Rac levels, suggesting that Rac activation was induced by TGF-β in these cells. In addition, NSC23766, a specific inhibitor of the activation of Rac (Gao et al., 2004), markedly upregulated the

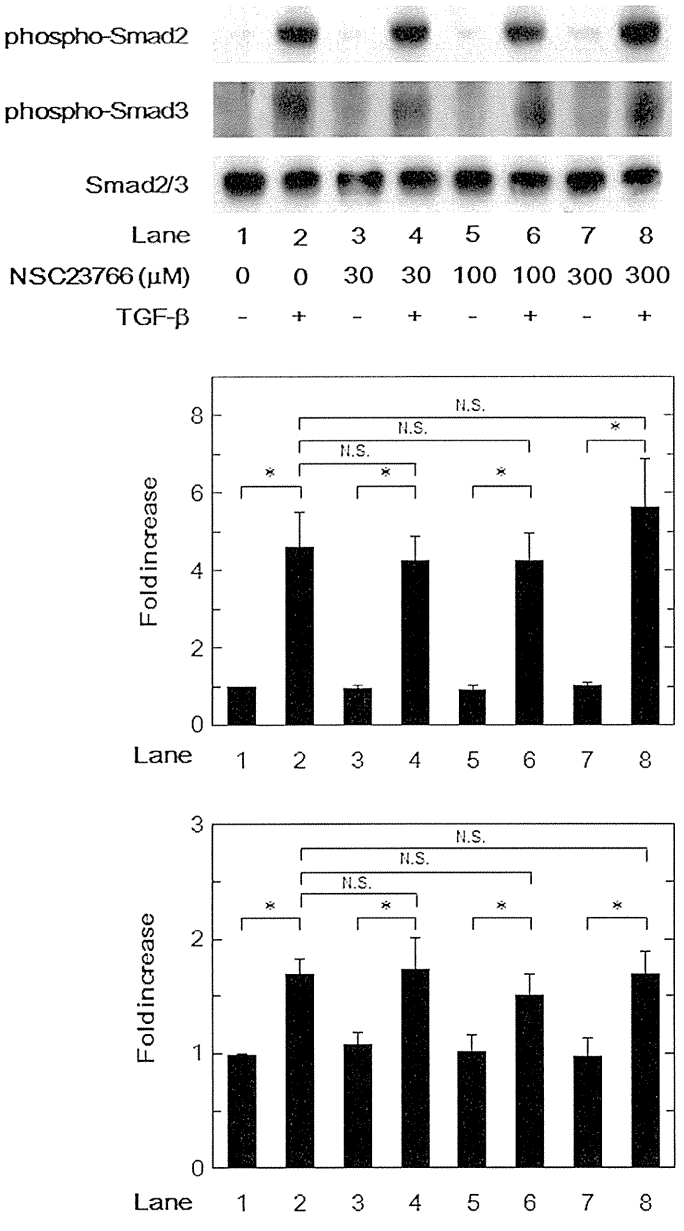

Fig. 4. Effects of NSC23766 on the TGF-β-induced phosphorylation of Smad2 and Smad3 in MC3T3-E1 cells. The cultured cells were pretreated with various doses of NSC23766 for 60 min, and then stimulated by 5 ng/ml of TGF-β or vehicle for 120 min. The cell extracts were then subjected to SDS-PAGE with a subsequent Western blot analysis with antibodies against phospho-specific Smad2, phospho-specific Smad3 or Smad2/3. The histogram shows a quantitative representation of the levels of TGF-β-induced phosphorylation obtained from a laser densitometric analysis of three independent experiments. Each value represents the mean ± SEM of triplicate determinations. $^{*}P < 0.05$, compared with the value of the control. N.S. designates no significant differences between the indicated pairs.

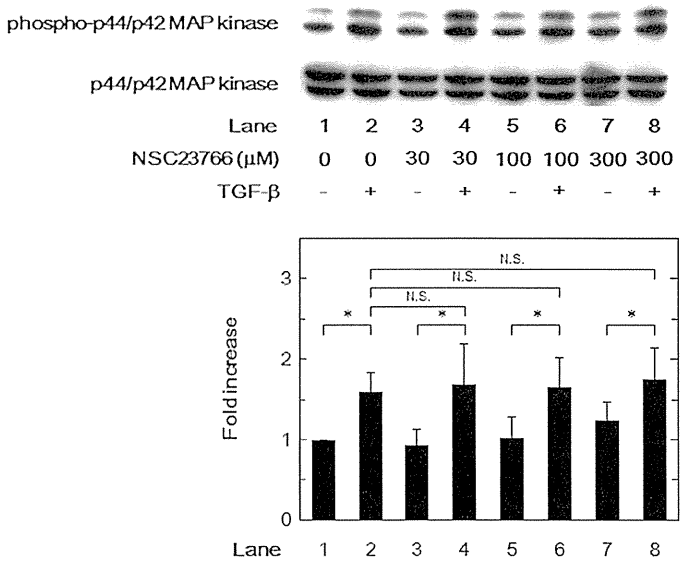

Fig. 5. Effect of NSC23766 on the TGF-β-induced phosphorylation of p44/p42 MAP kinase in MC3T3-E1 cells. The cultured cells were pretreated with various doses of NSC23766 for 60 min, and then stimulated by 5 ng/ml of TGF-β or vehicle for 120 min. The cell extracts were then subjected to SDS-PAGE with a subsequent Western blot analysis with antibodies against phospho-specific p44/p42 MAP kinase or p44/p42 MAP kinase. The histogram shows a quantitative representation of the levels of TGF-β-induced phosphorylation obtained from a laser densitometric analysis of three independent experiments. Each value represents the mean ± SEM of triplicate determinations. $^{*}P < 0.05$, compared with the value of the control. N.S. designates no significant differences between the indicated pairs.

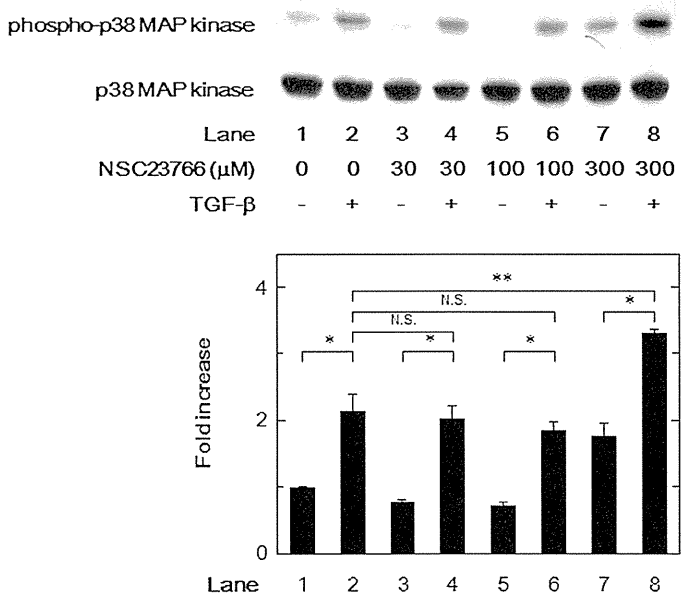

Fig. 6. Effect of NSC23766 on the TGF-β-induced phosphorylation of p38 MAP kinase in MC3T3-E1 cells. The cultured cells were pretreated with various doses of NSC23766 for 60 min, and then stimulated by 5 ng/ml of TGF-β or vehicle for 120 min. The cell extracts were then subjected to SDS-PAGE with a subsequent Western blot analysis with antibodies against phospho-specific p38 MAP kinase or p38 MAP kinase. The histogram shows a quantitative representation of the levels of TGF-β-induced phosphorylation obtained from a laser densitometric analysis of three independent experiments. Each value represents the mean ± SEM of triplicate determinations. $^{*}P < 0.05$, compared with the value of the control. $^{**}P < 0.05$, compared with the value of TGF-β alone. N.S. designates no significant differences between the indicated pairs.

TGF-β-stimulated VEGF release in these cells. Indeed, Fig. 2 showed a bell-shaped curve, indicating that the effect of NSC23766 at 300 μM was less than that at 200 μM. Regarding the effect of NSC23766 as a selective inhibitor of Rac-GEF interaction, the IC_{50} of NC23766 is reportedly under 50 μM (Gao et al., 2004). It is likely that higher concentrations of NSC23766 exert non-specific effects that deteriorate the specific amplifying effect on the TGF-β-stimulated VEGF synthesis in addition to the specific effect of NSC23766 as a Rac inhibitor in osteoblast-like MC3T3-E1 cells. Additionally, the VEGF release stimulated by TGF-β was amplified in the Rac-knock down MC3T3-E1 cells. These findings suggest that the Rac activated by

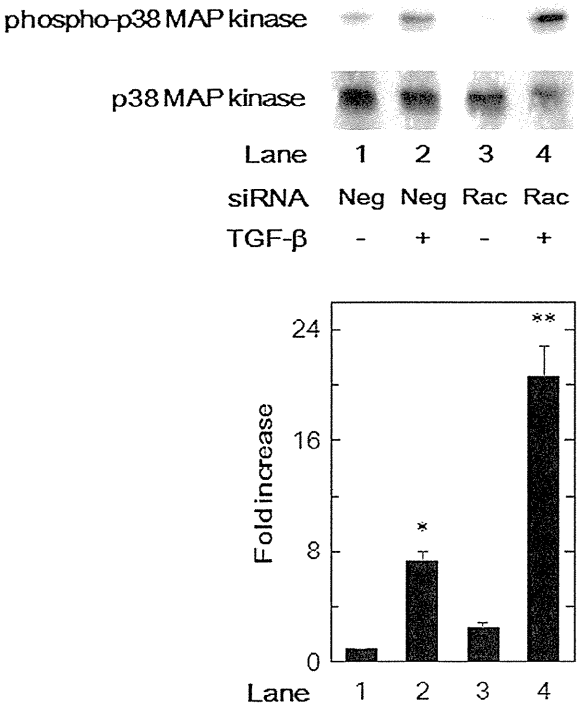

Fig. 7. Effect of TGF-β on the phosphorylation of p38 MAP kinase in the Rac-knock down MC3T3-E1 cells. The cultured cells were transfected with 50 nM of negative control siRNA (Neg) or 50 nM of Rac-siRNA (Rac) utilizing siLentFect as described in Section 2. The cells were then stimulated by 5 ng/ml of TGF-β or vehicle for 120 min. The cell extracts were subjected to SDS-PAGE with a subsequent Western blot analysis with antibodies against phospho-specific p38 MAP kinase or p38 MAP kinase. The histogram shows a quantitative representation of the levels of TGF-β-induced phosphorylation obtained from a laser densitometric analysis of three independent experiments. Each value represents the mean ± SEM of triplicate determinations. $^{*}P < 0.05$, compared with the value of vehicle with negative control siRNA transfection. $^{**}P < 0.05$, compared with the value of TGF-β with negative control siRNA transfection.

TGF-β acts as a negative regulator of the TGF-β-induced VEGF release in osteoblast-like MC3T3-E1 cells. We further demonstrated that the expression levels of VEGF mRNA induced by TGF-β were enhanced by NSC23766 in MC3T3-E1 cells. Therefore, it is probable that the negative regulation of the TGF-β-stimulated VEGF release by Rac is mediated through the transcriptional levels in these cells. As for osteoblasts, it has been shown that the inhibition of Rac reduces cell adhesion, spreading and proliferation in osteoblast-like MC3T3-E1 cells (Jung et al., 2011). In addition, it has been reported that the activation of Rac suppresses the bone morphogenetic protein-2-induced alkaline phosphatase activity in myoblastic C2C12 cells, suggesting the inhibitory role of Rac in osteoblastic differentiation (Onishi et al., 2013). To the best of our knowledge, the present report is probably the first report to clearly indicate the involvement of Rac in the TGF-β-stimulated VEGF synthesis in osteoblasts.

We next investigated the detailed mechanisms underlying the suppressive effect of Rac on the TGF-β-stimulated VEGF synthesis in osteoblast-like MC3T3-E1 cells. Important intracellular mediators of TGF-β signaling are Smad proteins, such as Smad2 and Smad3 (Miyazawa et al., 2002). We herein showed that SIS3, which selectively inhibits TGF-β-dependent Smad3 phosphorylation and Smad3-mediated cellular signaling (Jinnin et al., 2006), significantly decreased the TGF-β-stimulated VEGF release in MC3T3-E1 cells. Therefore, it is likely that the Smad-dependent pathway is involved in the TGF-β-stimulated VEGF release in these cells. However, NSC23766 had little effect on the TGF-β-induced phosphorylation of Smad2 and Smad3. Based on these findings, it is unlikely that the negative regulation of the TGF-β-induced VEGF synthesis by Rac is exerted through the Smad-dependent pathway in osteoblast-like MC3T3-E1 cells.

It is currently recognized that TGF-β exerts its effects on a variety of biological functions via the Smad-independent pathway, including the MAP kinase superfamily, in addition to the Smad-dependent pathway (Moustakas and Heldin, 2005). As for TGF-β intracellular signaling in osteoblasts, we have previously demonstrated that the TGF-β stimulated VEGF synthesis is positively regulated by p44/

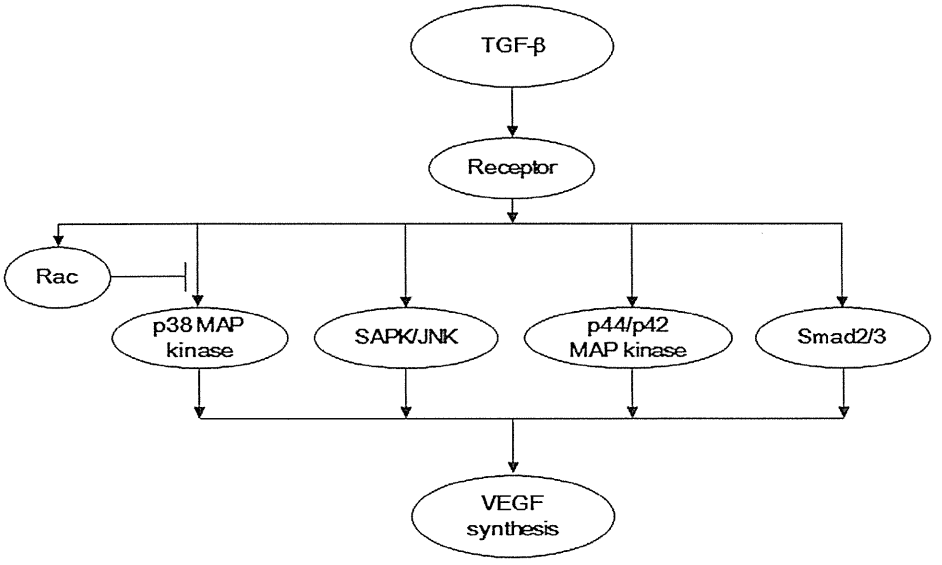

Fig. 8. Schematic illustration of the regulatory mechanism of Rac in the TGF-β-induced VEGF synthesis in MC3T3-E1 cells. TGF-β-activated Rac negatively regulates the TGF-β-stimulated VEGF synthesis via the suppression of p38 MAP kinase in osteoblast-like MC3T3-E1 cells.

p42 MAP kinase, p38 MAP kinase and SAPK/JNK in osteoblast-like MC3T3-E1 cells (Kanno et al., 2005; Tokuda et al., 2003). Therefore, we investigated whether Rac downregulates the synthesis of VEGF stimulated by TGF-β via the signaling of p44/p42 MAP kinase, p38 MAP kinase and/or SAPK/JNK in osteoblast-like MC3T3-E1 cells. We showed that NSC23766 markedly amplified the phosphorylation of p38 MAP kinase without affecting the phosphorylation of p44/p42 MAP kinase or SAPK/JNK in these cells. These findings suggest that the suppressive effect of Rac on the TGF-β-stimulated VEGF synthesis is mediated through the suppression of p38 MAP kinase, but not p44/p42 MAP kinase or SAPK/JNK in osteoblast-like MC3T3-E1 cells. Furthermore, we demonstrated that the phosphorylation of p38 MAP kinase induced by TGF-β was significantly strengthened in the Rac-knock down MC3T3-E1 cells with Rac-siRNA compared with that observed in the control cells. Taking our findings into account as a whole, it is most likely that Rac is activated by TGF-β and functions as a negative regulator in the TGF-β-stimulated VEGF synthesis and that the suppressive effect of Rac is exerted at a point upstream of p38 MAP kinase in osteoblast-like MC3T3-E1 cells. The possible regulatory mechanism of Rac in TGF-β-stimulated VEGF synthesis in osteoblasts is summarized in Fig. 8.

It is generally recognized that TGF-β promotes bone remodeling, a process initiated by osteoclastic bone resorption and subsequent osteoblastic bone formation (Janssens et al., 2005). TGF-β, which is embedded in the bone matrix and released during bone resorption, stimulates the synthesis of VEGF, a potent mitogen and angiogenic factor for vascular endothelial cells, in osteoblasts. This process is thought to play an important role in proper bone remodeling, which is essential for maintaining bone quality and bone mass. Our present results suggest that the predominant pathway in TGF-β-stimulated VEGF synthesis is the Smad3 pathway in osteoblasts and that the inhibition of Rac enhances VEGF synthesis via p38 MAP kinase independently of the Smad pathway. Taking these findings into account, it seems that Rac may play a role, at least in part, in regulating bone remodeling as a modulator of VEGF synthesis in osteoblasts. It is therefore possible that regulating the Rac activity in osteoblasts may provide a novel therapeutic strategy for treating metabolic bone diseases, such as osteoporosis. Further investigation is necessary to clarify the detailed mechanisms by which Rac regulates VEGF synthesis in osteoblasts.

In conclusion, our results strongly suggest that Rac limits the TGF-β-stimulated VEGF synthesis via the inhibition of p38 MAP kinase in osteoblasts.

Acknowledgements

We are very grateful to Yumiko Kurokawa for her skillful technical assistance. This investigation was supported in part by a Grant-in-Aid for Scientific Research (No. 19591042) from the Ministry of Education, Science, Sports and Culture of Japan and the Research Funding for Longevity Sciences (23-9, 25-4) from National Center for Geriatrics and Gerontology (NCGG), Japan.

References

Boyce, B.F., Xing, L., 2008. Functions of RANKL/RANK/OPG in bone modeling and remodeling. Arch. Biochem. Biophys. 473, 139–146.
Brandi, M.L., Collin-Osdoby, P., 2006. Vascular biology and the skeleton. J. Bone Miner. Res. 21, 183–192.
Clarkin, C.E., Gerstenfeld, L.C., 2013. VEGF and bone cell signalling: an essential vessel for communication? Cell Biochem. Funct. 31, 1–11.
Etienne-Manneville, S., Hall, A., 2002. Rho GTPases in cell biology. Nature 420, 629–635.
Ferrara, N., 2004. Vascular endothelial growth factor: basic science and clinical progress. Endocr. Rev. 25, 581–611.
Gao, Y., Dickerson, J.B., Guo, F., Zheng, J., Zheng, Y., 2004. Rational design and characterization of a Rac GTPase-specific small molecule inhibitor. Proc. Natl. Acad. Sci. U.S.A. 101, 7618–7623.
Guo, X., Wang, X.F., 2009. Signaling cross-talk between TGF-β/BMP and other pathways. Cell Res. 19, 71–88.
Janssens, K., ten Dijke, P., Janssens, S., Van Hul, W., 2005. Transforming growth factor-β1 to the bone. Endocr. Rev. 26, 743–774.
Jinnin, M., Ihn, H., Tamaki, K., 2006. Characterization of SIS3, a novel specific inhibitor of Smad3, and its effect on transforming growth factor-β1-induced extracellular matrix expression. Mol. Pharmacol. 69, 597–607.
Jung, G.Y., Park, Y.J., Han, J.S., 2011. Mediation of Rac1 activation by kindlin-2: an essential function in osteoblast adhesion, spreading, and proliferation. J. Cell. Biochem. 112, 2541–2548.
Kanno, Y., Ishisaki, A., Yoshida, M., Tokuda, H., Numata, O., Kozawa, O., 2005. SAPK/JNK plays a role in transforming growth factor-β-induced VEGF synthesis in osteoblasts. Horm. Metab. Res. 37, 140–145.
Karsenty, G., Wagner, E.F., 2002. Reaching a genetic and molecular understanding of skeletal development. Dev. Cell 2, 389–406.
Kato, K., Ito, H., Hasegawa, K., Inaguma, Y., Kozawa, O., Asano, T., 1996. Modulation of the stress-induced synthesis of hsp27 and alpha B-crystallin by cyclic AMP in C6 rat glioma cells. J. Neurochem. 66, 946–950.
Kozawa, O., Tokuda, H., Miwa, M., Kotoyori, J., Oiso, Y., 1992. Cross-talk regulation between cyclic AMP production and phosphoinositide hydrolysis induced by prostaglandin E2 in osteoblast-like cells. Exp. Cell Res. 198, 130–134.
Laemmli, U.K., 1970. Cleavage of structural proteins during the assembly of the head of bacteriophage T4. Nature 227, 680–685.
Miyazawa, K., Shinozaki, M., Hara, T., Furuya, T., Miyazono, K., 2002. Two major Smad pathways in TGF-β superfamily signalling. Genes Cells 7, 1191–1204.
Moustakas, A., Heldin, C.H., 2005. Non-Smad TGF-β signals. J. Cell Sci. 118, 3573–3584.
Onishi, M., Fujita, Y., Yoshikawa, H., Yamashita, T., 2013. Inhibition of Rac1 promotes BMP-2-induced osteoblastic differentiation. Cell Death Dis. 4, e698.
Saadeh, P.B., Mehrara, B.J., Steinbrech, D.S., Dudziak, M.E., Greenwald, J.A., Luchs, J.S., et al., 1999. Transforming growth factor-β1 modulates the expression of vascular endothelial growth factor by osteoblasts. Am. J. Physiol. 277, C628–C637.
Sudo, H., Kodama, H., Amagai, Y., Yamamoto, S., Kasai, S., 1983. In vitro differentiation and calcification in a new clonal osteogenic cell line derived from newborn mouse calvaria. J. Cell Biol. 96, 191–198.
ten Dijke, P., Hill, C.S., 2004. New insights into TGF-β-Smad signalling. Trends Biochem. Sci. 29, 265–273.
Takai, Y., Sasaki, T., Matozaki, T., 2001. Small GTP-binding proteins. Physiol. Rev. 81, 153–208.
Tang, Y., Wu, X., Lei, W., Pang, L., Wan, C., Shi, Z., et al., 2009. TGF-β1-induced migration of bone mesenchymal stem cells couples bone resorption with formation. Nat. Med. 15, 757–765.
Tokuda, H., Hatakeyama, D., Akamatsu, S., Tanabe, K., Yoshida, M., Shibata, T., et al., 2003. Involvement of MAP kinases in TGF-β-stimulated vascular endothelial growth factor synthesis in osteoblasts. Arch. Biochem. Biophys. 415, 117–125.
Zelzer, E., Olsen, B.R., 2005. Multiple roles of vascular endothelial growth factor (VEGF) in skeletal development, growth, and repair. Curr. Top. Dev. Biol. 65, 169–187.
Zuo, C., Huang, Y., Bajis, R., Sahih, M., Li, Y.P., Dai, K., et al., 2012. Osteoblastogenesis regulation signals in bone remodeling. Osteoporos. Int. 23, 1653–1663.

Article outline Show full outline

Figures and tables

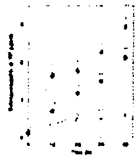

Table 1

Table 2

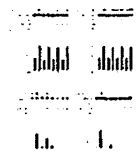

Prostaglandins & Other Lipid Mediators

Volumes 116–117, January–March 2015, Pages 57–63

86174||
Original Research Article

Resveratrol reduces prostaglandin E_1-stimulated osteoprotegerin synthesis in osteoblasts: Suppression of stress-activated protein kinase/c-Jun N-terminal kinase

Naohiro Yamamoto[a, b], Takanobu Otsuka[a], Gen Kuroyanagi[a, b], Akira Kondo[a, b], Shingo Kainuma[a, b], Akira Nakakami[b], Rie Matsushima-Nishiwaki[b], Osamu Kozawa[b], Haruhiko Tokuda[b, c]

Show more

doi:10.1016/j.prostaglandins.2015.01.003

Highlights

- Resveratrol suppresses OPG release induced by PGE_1 and the mRNA expression.
- SRT1720, an activator of SIRT1, reduces the release of OPG.
- Resveratrol and SRT1720 attenuate PGE_1-induced phosphorylation of SAPK/JNK.
- Resveratrol inhibits PGE_1-stimulated OPG synthesis via suppression of SAPK/JNK in osteoblasts.

Abstract

Resveratrol, a natural polyphenol mainly existing in red grapes and berries, possesses beneficial effects on human being. We have previously reported that prostaglandin E_1 (PGE_1) stimulates vascular endothelial growth factor synthesis via activation of p38 mitogen-activated protein (MAP) kinase and stress-activated protein kinase/c-Jun N-terminal kinase (SAPK/JNK) but not p44/p42 MAP kinase in osteoblast-like MC3T3-E1 cells. In the present study, we investigated the PGE_1-effect on osteoprotegerin (OPG) synthesis and the effect of resveratrol on the synthesis in MC3T3-E1 cells. PGE_1 induced the expression levels of OPG mRNA and stimulated the OPG release. Resveratrol significantly reduced the PGE_1-induced OPG release and the mRNA expression. SRT1720, an activator of SIRT1, suppressed the release of OPG. The protein levels of SIRT1 were not up-regulated by resveratrol with or without PGE_1. Both SB203580 and SP600125, a specific p38 MAP kinase inhibitor and a specific SAPK/JNK inhibitor, respectively, but not PD98059, a specific MEK inhibitor, reduced the PGE_1-stimulated OPG release. Resveratrol or SRT1720 failed to affect the phosphorylation of p38 MAP kinase. On the contrary, PGE_1-induced phosphorylation of SAPK/JNK was significantly attenuated by both resveratrol and SRT1720. Our results strongly suggest that resveratrol inhibits PGE_1-stimulated OPG synthesis via suppressing SAPK/JNK but not p38 MAP kinase in osteoblasts.

Keywords

Resveratrol; PGE_1; SAPK/JNK; Osteoprotegerin; Osteoblast

1. Introduction

Osteoprotegerin (OPG), a glycoprotein that belongs to the tumor necrosis factor receptor superfamily, is well recognized to possess inhibitory effects on osteoclast activation along with receptor activator of nuclear factor κB (RANK) [1]. Bone metabolism is regulated mainly by two functional cells, osteoblasts and osteoclasts responsible for bone formation and bone resorption, respectively [2]. The formation of bone structures and bone remodeling result from the sophisticated coupling process of osteoblasts and osteoclasts. The disorder of bone remodeling causes metabolic bone disorders such as osteoporosis and fracture healing distress. In proceeding of bone remodeling, it is generally recognized that numerous humoral factors including prostaglandins and cytokines play pivotal roles [3]. In response to numerous hormones, cytokines and prostaglandins, osteoblasts produce RANK ligand (RANKL) and OPG [3]. OPG binds to RANKL as a decoy receptor and inhibits the binding of RANKL to RANK, an essential step of osteoclastogenesis for osteoclast-precursor cells derived from macrophages [4]. It has been reported that RANKL-knock out mice are suffered from severe osteopetrosis, suggesting that RANKL is a central regulator of osteoclastogenesis [5]. It is currently recognized that the RANK/RANKL/OPG axis is an important regulatory system for the function of osteoclasts.

It is firmly established that prostaglandins act as local factors, autacoids, in bone metabolism, and play an important role in bone cell function. Among them, prostaglandin E_1 (PGE_1) is recognized as a potent bone-

resorptive agent in the control of bone anabolism [6]. In our previous studies [7] and [8], we have shown that PGE_1 stimulates the synthesis of vascular endothelial growth factor via p38 mitogen-activated protein (MAP) kinase and stress-activated protein kinase/c-Jun N-terminal kinase (SAPK/JNK) but not p44/p42 MAP kinase in osteoblast-like MC3T3-E1 cells. However, the exact role of PGE_1 in osteoblasts remains to be elucidated.

Polyphenolic compounds in foods such as vegetables and fruits have beneficial properties for human being. Among them, flavonoids show antioxidative, antiinflammatory and anticarcinogenic effects [9] and [10]. The consumption of resveratrol, a natural polyphenolic flavonoid enriched in red grapes and berries, reportedly improves health and prolongs life [11]. It is well known that there is low mortality from coronary heart disease in France with many amount of wine consumption containing abundant resveratrol [12]. It has been shown that resveratrol increases life span in lower organisms by activating the nicotinamide adenine dinucleotide (NAD^+)-dependent histone deacetylase SIRT1 [13]. NAD^+ is biosynthesized in the body as a precursor of nicotinamide, and has an important role for energy acquisition as a coenzyme of oxidoreductase. SIRT1 has been identified as a transcriptional silencer in yeast and modulates the pathways downstream of caloric restriction that produces beneficial effects for mammals [11]. However, the details of resveratrol actions on bone metabolism have not yet been clarified.

In the present study, we investigated the mechanism of OPG synthesis induced by PGE_1 and the effect of resveratrol on the OPG synthesis in osteoblast-like MC3T3-E1 cells. We herein demonstrate that resveratrol suppresses PGE_1-stimulated OPG synthesis through inhibiting activation of SAPK/JNK in osteoblasts.

2. Materials and methods

2.1. Materials

Resveratrol, SRT1720, PD98059, SB203580 and SP600125 were obtained from Calbiochem-Novabiochem Co. (La Jolla, CA). PGE_1 was obtained from Sigma Chemical Co. (St. Louis, MO). A mouse OPG enzyme-linked immunosorbent assay (ELISA) kit was obtained from R&D Systems, Inc. (Minneapolis, MN). Phospho-specific p38 MAP kinase antibodies, p38 MAP kinase antibodies, phospho-specific SAPK/JNK antibodies, SAPK/JNK antibodies and SIRT1 antibodies were obtained from Cell Signaling, Inc. (Beverly, MA). Glyceraldehyde-3-phosphate dehydrogenase (GAPDH) antibodies were obtained from Santa Cruz Biotechnology (Santa Cruz, CA). An ECL Western blotting detection system was obtained from GE Healthcare (Buckinghamshire, UK). Other materials and chemicals were obtained from commercial sources. PGE_1 was dissolved in ethanol. Resveratrol, SRT1720, PD98059, SB203580 and SP600125 were dissolved in dimethyl sulfoxide. The maximum concentration of ethanol or dimethyl sulfoxide was 0.1%, which did not affect either the assay for OPG or the detection of the protein level using Western blot analysis.

2.2. Cell culture

Cloned osteoblast-like MC3T3-E1 cells that have been derived from newborn mouse calvaria [14] were maintained as previously described [15]. Briefly, the cells were cultured in α-minimum essential medium (α-MEM) containing 10% fetal bovine serum (FBS) at 37 °C in a humidified atmosphere of 5% CO_2/95% air. The cells were seeded into 35-mm diameter dishes (5×10^4 cells/dish) or 90-mm diameter dishes (2×10^5 cells/dish) in α-MEM containing 10% FBS. After 5 days, the medium was exchanged for α-MEM containing 0.3% FBS. The cells were used for experiments after 48 h.

2.3. Assay for OPG

The cultured cells were pretreated with various doses of resveratrol, SRT1720, PD98059, SB203580 or SP600125 for 60 min, and then stimulated by 10 μM of PGE_1 or vehicle in 1 ml of α-MEM containing 0.3% FBS for the indicated periods. The conditioned medium was collected at the end of incubation, and the OPG concentration was then measured using the OPG ELISA kit according to the manufacturer's protocol. The viability of cells stimulated by 10 μM of PGE_1 for 48 h with 1 h-pretreatment of 50 μM of resveratrol, 10 μM of SRT1720, 30 μM of SB203580 or 10 μM of SP600125 was above 97% compared to that without pretreatment by trypan blue dye exclusion test.

2.4. Real-time RT-PCR

The cultured cells were pretreated with 50 μM of resveratrol, 10 μM of SRT1720 or vehicle for 60 min, and then stimulated by 10 μM of PGE_1 or vehicle in α-MEM containing 0.3% FBS for 3 h. Total RNA was isolated and transcribed into complementary DNA using Trizol reagent (Invitrogen Corp., Carlsbad, CA) and Omniscript Reverse Transcriptase kit (QIAGEN Inc., Valencia, CA), respectively. Real-time RT-PCR was performed using a Light Cycler system in capillaries and Fast Start DNA Master SYBR Green I provided with the kit (Roche Diagnostics, Basel, Switzerland). Sense and antisense primers for mouse OPG mRNA or GAPDH mRNA were purchased from Takara Bio Inc. (Tokyo, Japan) (primer set ID: MA026526). The amplified products were determined using a melting curve analysis and agarose electrophoresis. The OPG mRNA levels were normalized to those of GAPDH mRNA.

2.5. Western blot analysis

The cultured cells were pretreated with various doses of resveratrol or SRT1720 for 60 min, and then stimulated by PGE_1 in α-MEM containing 0.3% FBS for the indicated periods. The cells were washed twice with phosphate-buffered saline and then lysed, homogenized and sonicated in a lysis buffer containing 62.5 mM Tris/HCl, pH 6.8, 2% sodium dodecyl sulfate (SDS), 50 mM dithiothreitol and 10% glycerol. SDS-

polyacrylamide gel electrophoresis (PAGE) was performed by the method of Laemmli [16] in 10% polyacrylamide gels. The protein was fractionated and transferred onto an Immun-Blot PVDF Membrane (Bio-Rad, Hercules, CA). The membranes were blocked with 5% fat-free dry milk in Tris-buffered saline-Tween (TBS-T; 20 mM Tris-HCl, pH 7.6, 137 mM NaCl, 0.1% Tween 20) for 2 h before incubation with primary antibodies. A Western blot analysis was performed as described previously [17] using phospho-specific p38 MAP kinase antibodies, p38 MAP kinase antibodies, phospho-specific SAPK/JNK antibodies, SAPK/JNK antibodies, SIRT1 antibodies or GAPDH antibodies as primary antibodies with peroxidase-labeled antibodies raised in goat against rabbit IgG being used as secondary antibodies. The primary and secondary antibodies were diluted at 1:1000 with 5% fat-free dry milk in TBS-T. The peroxidase activity on the PVDF sheet was visualized on X-ray film by means of the ECL Western blotting detection system.

2.6. Determination of densitometric analysis

Densitometric analysis was performed using scanner and image analysis software (image J version 1.45). The phosphorylated protein levels were calculated as follows: the background-subtracted signal intensity of each phosphorylation signal was normalized to the respective total protein signal and plotted as the fold increase in comparison to control cells without stimulation.

2.7. Statistical analysis

The data were analyzed by ANOVA followed by Bonferroni method for multiple comparisons between pairs, and $p < 0.05$ was considered to be statistically significant. All data are presented as the mean ± S.E.M. of triplicate determinations from three independent cell preparations.

3. Results

3.1. Effect of resveratrol on the PGE_1-stimulated OPG release in MC3T3-E1 cells

In order to investigate whether PGE_1 stimulates OPG synthesis or not in osteoblast-like MC3T3-E1 cells, we examined the effect of PGE_1 on the OPG release. PGE_1 significantly increased the release of OPG in a time-dependent manner up to 48 h (Fig. 1). In addition, we examined the effect of resveratrol on the PGE_1-stimulated OPG release in these cells. Resveratrol, which alone had little effect on the basal levels of OPG, significantly reduced the PGE_1-stimulated OPG release in a dose-dependent manner in the range between 10 and 70 μM (Fig. 2). The maximum effect of resveratrol on the release was observed at 70 μM, which caused an approximate 45% decrease in the PGE_1-effect.

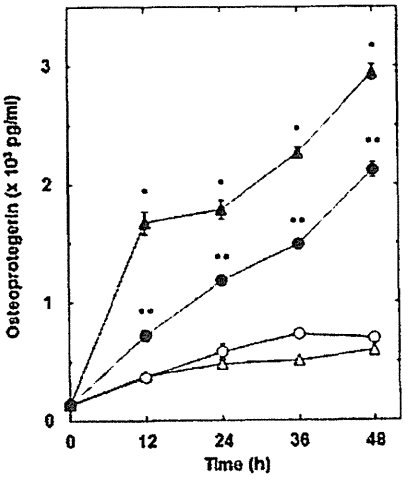

Fig. 1.

Effect of resveratrol on the PGE_1-stimulated OPG release in MC3T3-E1 cells. The cultured cells were pretreated with 50 μM of resveratrol (•, ▲) or vehicle (○, △) for 60 min, and then stimulated by 10 μM of PGE_1 (•, ▲) or vehicle (○, △) for the indicated periods. The OPG concentrations of the conditioned mediums were determined by ELISA. Each value represents the mean + S.E.M. of triplicate determinations from three independent cell preparations. $^{*}p < 0.05$ compared to the value of control $^{**}p < 0.05$ compared to the value of PGE_1 alone.

Figure options

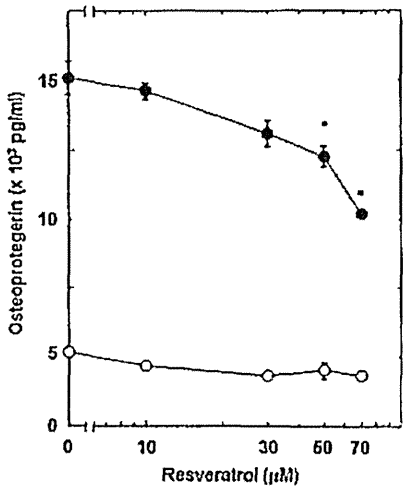

Fig. 2.

Dose-dependent effect of resveratrol on the PGE_1-stimulated OPG release in MC3T3-E1 cells. The cultured cells were pretreated with various doses of resveratrol for 60 min, and then stimulated by 10 μM of PGE_1 (•) or vehicle (○) for 48 h. The OPG concentrations of the conditioned mediums were determined by ELISA. Each value represents the mean ± S.E.M. of triplicate determinations from three independent cell preparations. *$p < 0.05$, compared to the value of PGE_1 alone.

Figure options

3.2. Effect of SRT1720 on the PGE_1-stimulated OPG release in MC3T3-E1 cells

It is generally known that SRT1720 is an activator of SIRT1 as well as resveratrol [18]. Therefore, we next examined the effect of SRT1720 on the PGE_1-stimulated OPG release in MC3T3-E1 cells. SRT1720 significantly suppressed the PGE_1-stimulated OPG release (Table 1). The inhibitory effect of SRT1720 at 10 μM caused a 35% decrease in the PGE_1-effect.

Table 1.

Effect of SRT1720 on the PGE_1-stimulated OPG release in MC3T3-E1 cells.

SRT1720	PGE_1	OPG (pg/ml)
–	–	848 ± 16
–	+	3800 ± 106*
+	–	741 ± 33
+	+	2657 ± 79**

The cultured cells were pretreated with 10 μM of SRT1720 or vehicle for 60 min, and then stimulated by 10 μM of PGE_1 or vehicle for 48 h. The OPG concentrations in the conditioned mediums were determined by ELISA. Each value represents the mean ± S.E.M. of triplicate determinations from three independent cell preparations.

* $p < 0.05$, compared to the value of control.

** $p < 0.05$, compared to the value of PGE_1 alone.

Table options

3.3. Effects of resveratrol or SRT1720 on the PGE_1-induced expression levels of OPG mRNA in MC3T3-E1 cells

In order to explore whether the suppressing effects of resveratrol or SRT1720 on PGE_1-stimulated OPG release are meditated through transcriptional events or not, we further examined the effects of resveratrol or SRT1720 on the PGE_1-induced OPG mRNA expression by real-time RT-PCR. As well as the PGE_1-stimulated OPG release, resveratrol markedly reduced the expression levels of OPG mRNA induced by PGE_1 (Fig. 3A). In addition, the PGE_1-elicited OPG mRNA expression levels were significantly suppressed by 10 μM of SRT1720 (Fig. 3B).

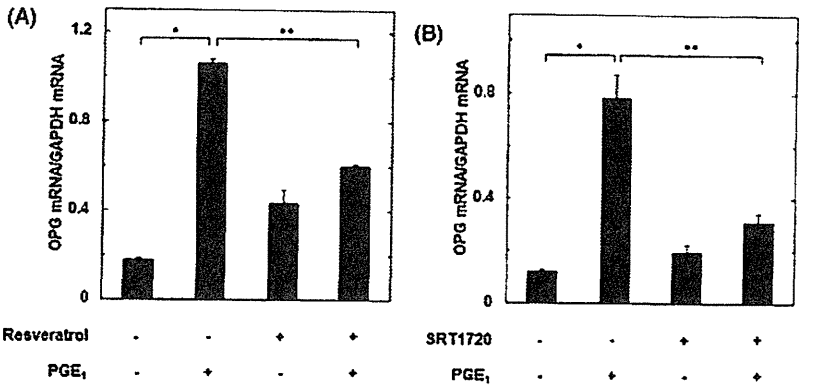

Fig. 3.

Effects of resveratrol (A) or SRT1720 (B) on the PGE_1-induced OPG mRNA expression in MC3T3-E1 cells. The cultured cells were pretreated with 50 μM of resveratrol, 10 μM of SRT1720 or vehicle for 60 min, and then stimulated by 10 μM of PGE_1 or vehicle for 3 h. The respective total RNA was then isolated and transcribed into cDNA. The expressions of OPG mRNA and GAPDH mRNA were quantified by real-time RT-PCR. The OPG mRNA levels were normalized to those of GAPDH mRNA. Each value represents the mean ± S.E.M. of triplicate determinations from three independent cell preparations. $^{*}p < 0.05$, compared to the value of control. $^{**}p < 0.05$, compared to the value of PGE_1 alone.

Figure options

3.4. Effects of resveratrol and/or PGE_1 on the levels of SIRT1 protein in MC3T3-E1 cells

To elucidate whether resveratrol and/or PGE_1 affect the SIRT1 expression in osteoblast-like MC3T3-E1 cells, we examined the effects of resveratrol and/or PGE_1 on the SIRT1 protein levels. We found that the expression of SIRT1 protein was observed in the unstimulated MC3T3-E1 cells, and the levels were not up-regulated by resveratrol with or without PGE_1 up to 48 h. In addition, the expression levels of SIRT1 protein were significantly decreased by resveratrol alone at 36 h and 48 h after the treatment (Fig. 4).

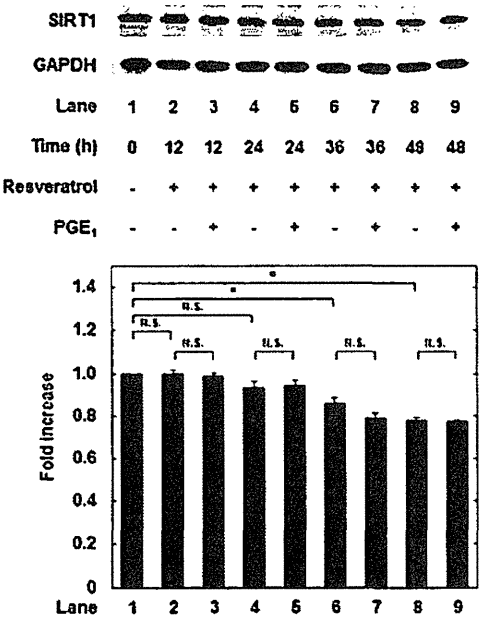

Fig. 4.

Effects of resveratrol and/or PGE_1 on the levels of SIRT1 protein in MC3T3-E1 cells. The cultured cells were pretreated with 50 μM of resveratrol or vehicle for 60 min, and then stimulated by 10 μM of PGE_1 or vehicle for the indicated periods. The cell extracts were then subjected to SDS-PAGE with subsequent Western blot analysis with antibodies against SIRT1 or GAPDH. The histogram shows quantitative representation of the levels of SIRT1 protein obtained from a laser densitometric analysis of three independent experiments. The protein levels of SIRT1 were corrected by the GAPDH levels. The protein levels were expressed as the fold increase to the basal levels presented as lane 1. Each value represents the mean ± S.E.M. of triplicate determinations. $^{*}p < 0.05$, compared to the value of control. N.S. designates no significant difference between the indicated pairs.

Figure options

3.5. Effects of PD98059, SB203580 and SP600125 on the PGE_1-stimulated OPG release in MC3T3-E1 cells

It is generally established that major MAP kinases such as p44/p42 MAP kinase, p38 MAP kinase and SAPK/JNK among the MAP kinase superfamily are intracellular signaling molecules used by mammalian cells to transduce a variety types of extracellular stimuli [19]. As for PGE_1-induced intracellular signaling in osteoblasts, we have previously shown that these three MAP kinases are activated by PGE_1 in osteoblast-like MC3T3-E1 cells [7] and [8]. In order to clarify whether p44/p42 MAP kinase, p38 MAP kinase or SAPK/JNK in MC3T3-E1 cells is involved in the PGE_1-stimulated OPG synthesis, we examined the effects

of PD98059, a specific inhibitor of the upstream kinase that activates p44/p42 MAP kinase [20], SB203580, a specific inhibitor of p38 MAP kinase [21], or SP600125, a specific inhibitor of SAPK/JNK [22], on the OPG release stimulated by PGE_1. SB203580 and SP600125 but not PD98059 significantly suppressed the PGE_1-stimulated OPG release (Table 2).

Table 2
Effects of PD98059, SB203580 or SP600125 on the PGE_1-stimulated OPG release in MC3T3-E1 cells.

Inhibitors	PGE_1	OPG (pg/ml)
–	–	1056 ± 22
–	+	4709 ± 190*
PD98059	–	1347 ± 58
PD98059	+	5332 ± 176
SB203580	–	582 ± 66
SB203580	+	1397 ± 43**
SP600125	–	990 ± 64
SP600125	+	3219 ± 150**

The cultured cells were pretreated with 50 μM of PD98059, 30 μM of SB203580, 10 μM of SP600125 or vehicle for 60 min, and then stimulated by 10 μM of PGE_1 or vehicle for 48 h. The OPG concentrations of the conditioned mediums were determined by ELISA. Each value represents the mean ± S.E.M. of triplicate determinations from three independent cell preparations.

* $p < 0.05$, compared to the value of control.

** $p < 0.05$, compared to the value of PGE_1 alone.

Table options

3.6. Effects of resveratrol or SRT1720 on the PGE_1-induced phosphorylation of p38 MAP kinase in MC3T3-E1 cells

In order to elucidate whether the suppressive effect of resveratrol on the PGE_1-stimulated OPG synthesis is mediated by the modulation of p38 MAP kinase activation in osteoblast-like MC3T3-E1 cells, we examined the effect of resveratrol on the PGE_1-induced phosphorylation of p38 MAP kinase. We previously reported that PGE_1 stimulates the phosphorylation of p38 MAP kinase in a time-dependent manner, and the maximum stimulatory effect is observed at 10 min [7]. Therefore, in the present study, we examined the effects of resveratrol or SRT1720 on the phosphorylation of p38 MAP kinase induced by PGE_1 for 10 min. Resveratrol failed to affect the PGE_1-induced phosphorylation of p38 MAP kinase in the range between 10 and 50 μM (Fig. 5A). In addition, SRT1720 had little effect on the p38 MAP kinase phosphorylation by PGE_1 as well as resveratrol (Fig. 5B).

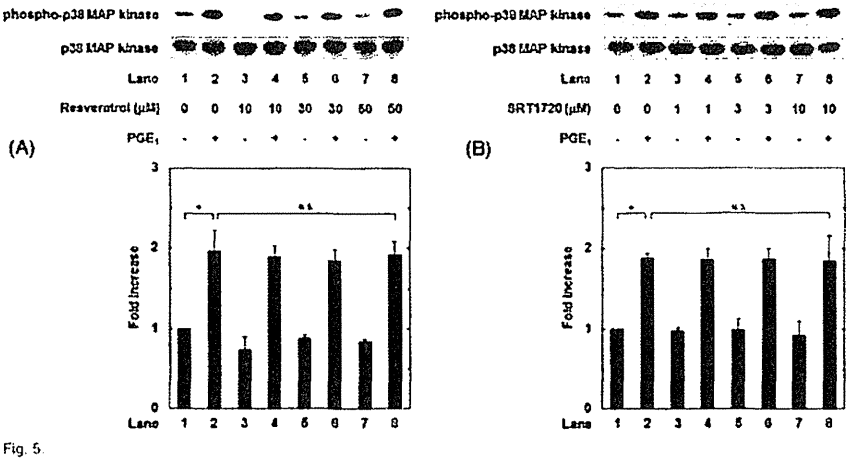

Fig. 5.
Effects of resveratrol (A) or SRT1720 (B) on the PGE_1-induced phosphorylation of p38 MAP kinase in MC3T3-E1 cells. The cultured cells were pretreated with various doses of resveratrol or SRT1720 for 60 min, and then stimulated by 10 μM of PGE_1 or vehicle for 10 min. The cell extracts were then subjected to SDS-PAGE with subsequent Western blot analysis with antibodies against phospho-specific p38 MAP kinase or p38 MAP kinase. The histogram shows quantitative representation of the levels of PGE_1-induced phosphorylation obtained from a laser densitometric analysis of three independent experiments. The phosphorylation levels were expressed as the fold increase to the basal levels presented as lane 1. Each value represents the mean ± S.E.M. of triplicate determinations. *$p < 0.05$, compared to the value of control. N.S. designates no significant difference between the indicated pairs.

Figure options

3.7. Effects of resveratrol or SRT1720 on the PGE_1-induced phosphorylation of SAPK/JNK in MC3T3-E1 cells

To investigate whether the resveratrol-effect on the PGE_1-stimulated OPG synthesis is mediated through SAPK/JNK activation in MC3T3-E1 cells, we next examined the effect of resveratrol on the PGE_1-induced phosphorylation of SAPK/JNK. We previously demonstrated that PGE_1 stimulates the phosphorylation of

SAPK/JNK in a time-dependent manner, and the effect reaches a plateau at 20 min [8]. Thus, we examined the effects of resveratrol or SRT1720 on the phosphorylation of SAPK/JNK induced by PGE_1 for 20 min. Resveratrol significantly reduced the PGE_1-induced phosphorylation of SAPK/JNK in a dose-dependent manner in the range between 10 and 50 μM (Fig. 6A).

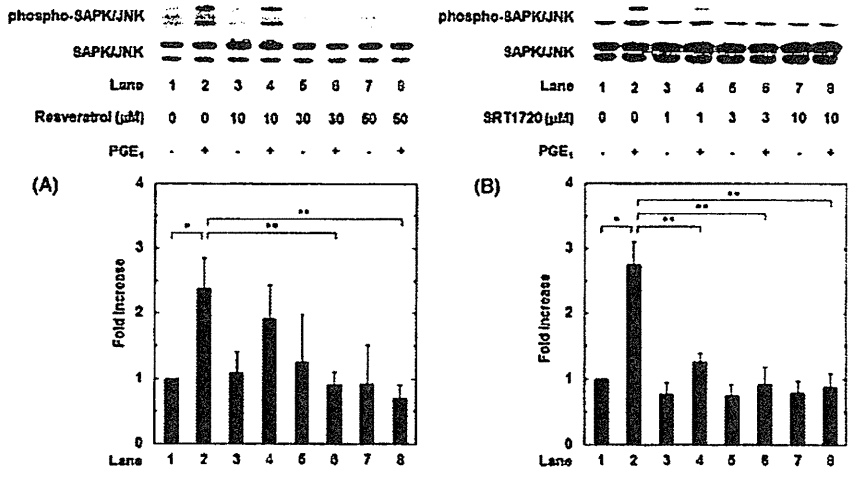

Fig. 6.

Effects of resveratrol (A) or SRT1720 (B) on the PGE_1-induced phosphorylation of SAPK/JNK in MC3T3-E1 cells. The cultured cells were pretreated with various doses of resveratrol or SRT1720 for 60 min, and then stimulated by 10 μM of PGE_1 or vehicle for 20 min. The cell extracts were then subjected to SDS-PAGE with subsequent Western blot analysis with antibodies against phospho-specific SAPK/JNK or SAPK/JNK. The histogram shows quantitative representation of the levels of PGE_1-induced phosphorylation obtained from a laser densitometric analysis of three independent experiments. The phosphorylation levels were expressed as the fold increase to the basal levels presented as lane 1. Each value represents the mean ± S.E.M. of triplicate determinations. $^{*}p < 0.05$, compared to the value of control. $^{**}p < 0.05$, compared to the value of PGE_1 alone.

Figure options

In order to clarify whether the inhibitory effect of resveratrol on the PGE_1-stimulated OPG synthesis is mediated through SIRT1 activation in MC3T3-E1 cells, we furthermore examined the effect of SRT1720 on the PGE_1-induced phosphorylation of SAPK/JNK. SRT1720 significantly attenuated the PGE_1-induced phosphorylation of SAPK/JNK in a dose-dependent manner in the range between 1 and 10 μM (Fig. 6B). Therefore, our findings suggest that SRT1720 mimics the effect of resveratrol on the PGE_1-induced phosphorylation of SAPK/JNK.

4. Discussion

In the present study, we showed that resveratrol significantly decreased the PGE_1-stimulated OPG release in osteoblast-like MC3T3-E1 cells. In addition, we demonstrated that PGE_1 up-regulated the expression levels of OPG mRNA, and resveratrol reduced the OPG mRNA levels in these cells. Therefore, our findings suggest that the inhibitory effect of resveratrol on PGE_1-stimulated OPG release is exerted at a point upstream of transcriptional levels on osteoblast-like MC3T3-E1 cells. It has been reported that several effects of resveratrol are dependent on SIRT1 activation [23]. We next showed that SRT1720 inhibited the PGE_1-stimulated OPG release and the OPG mRNA expression levels as well as resveratrol. SRT1720 is a synthetic compound that activates SIRT1 with potencies 1000-fold greater than resveratrol [18]. Thus, we speculate that resveratrol and SRT1720 share common pathway. Taking our findings into account, it is most likely that the suppressing effect of resveratrol on the PGE_1-induced OPG synthesis is mediated at least in part by the activation of SIRT1 in osteoblast-like MC3T3-E1 cells. On the other hand, we found that the protein levels of SIRT1 were not up-regulated by resveratrol with or without PGE_1, and that resveratrol alone significantly decreased the levels. It seems unlikely that the effect of resveratrol on PGE_1-induced OPG synthesis is caused by the up-regulation of SIRT1 protein expression. It is recognized that sirtuins including SIRT1 are NAD^+-dependent histone deacetylases, and that SIRT1 exerts its action by deacetylation on the target proteins in various tissues [24]. Therefore, it is possible that resveratrol might increase the deacetylation activity but not the expression of SIRT1 in osteoblast-like MC3T3-E1 cells, resulting in the suppression of PGE_1-stimulated OPG synthesis.

We next investigated the mechanism underlying PGE_1-induced OPG synthesis and the inhibitory effect of resveratrol in osteoblast-like MC3T3-E1 cells. Regarding the PGE_1-induced intracellular signaling in osteoblasts, we have previously reported that PGE_1 stimulates the activation of three major MAP kinases, p44/p42 MAP kinase, p38 MAP kinase and SAPK/JNK in osteoblast-like MC3T3-E1 cells, and that p38 MAP kinase and SAPK/JNK but not p44/p42 MAP kinase act as positive regulators in the PGE_1-stimulated synthesis of vascular endothelial growth factor [7] and [8]. Thus, in the present study, in order to investigate the involvement of three MAP kinases in the OPG synthesis in MC3T3-E1 cells, we examined the effects of three MAP kinase inhibitors, PD98059 [20], SB203580 [21] and SP600125 [22], on the PGE_1-stimulated OPG release. We demonstrated that SB203580 and SP600125 significantly reduced the PGE_1-stimulated OPG release whereas PD98059 failed to affect the release. Therefore, our results suggest that not p44/p42 MAP kinase but p38 MAP kinase and SAPK/JNK function as positive regulators in the PGE_1-stimulated OPG synthesis in osteoblast-like MC3T3-E1 cells.

In addition, in order to explore the exact mechanism how resveratrol inhibits the PGE_1-stimulated OPG

synthesis in osteoblast-like MC3T3-E1 cells, we examined the effects of resveratrol on the PGE_1-induced phosphorylation of p38 MAP kinase and SAPK/JNK. We here showed that resveratrol markedly suppressed the PGE_1-induced phosphorylation of SAPK/JNK without affecting the p38 MAP kinase phosphorylation. Based on our findings, it is probable that the suppressing effect of resveratrol on the PGE_1-stimulated OPG synthesis is mediated through inhibiting activation of SAPK/JNK in osteoblast-like MC3T3-E1 cells. In these MC3T3-E1 cells, we have recently shown that resveratrol down-regulates prostaglandin D_2-stimulated OPG synthesis through inhibiting p38 MAP kinase and SAPK/JNK [25], and that the OPG synthesis induced by prostaglandin $F_{2\alpha}$ is attenuated by resveratrol through the suppression of p44/p42 MAP kinase, p38 MAP kinase and SAPK/JNK [26]. It is recognized that signaling of PGE_1, PGD_2 and $PGF_{2\alpha}$ is mediated through the distinct G-protein-coupled receptor, EP, DP and FP, respectively, and that the signal transduction mechanisms are quite different from each other [27]. It is probable that the discrepancies between the present findings and these previous studies are due to the difference in ligand binding profiles among these specific receptors and the following signaling mechanism in osteoblasts. Furthermore, SRT1720 mimicked the inhibitory effect of resveratrol on the PGE_1-induced phosphorylation of SAPK/JNK without affecting p38 MAP kinase phosphorylation in these cells. Taking our findings into account, it is most likely that the effect of resveratrol on the PGE_1-stimulated OPG synthesis is mediated at least in part through activation of SIRT1 without up-regulating the expression in osteoblast-like MC3T3-E1 cells. The potential mechanism of resveratrol in PGE_1-stimulated OPG synthesis in osteoblasts shown here is summarized in Fig. 7.

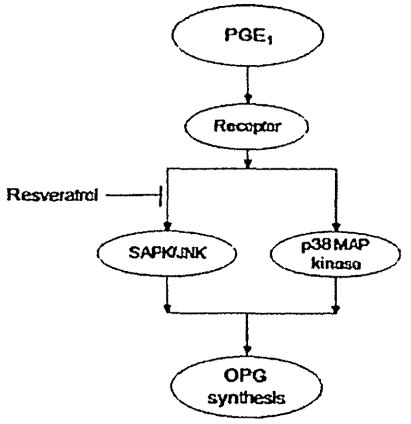

Fig. 7.

Schematic illustration of the regulatory mechanism of PGE_1-induced OPG synthesis and the inhibitory effect of resveratrol in osteoblast-like MC3T3-E1 cells. PGE_1, prostaglandin E_1; SAPK/JNK, stress-activated protein kinase/c-Jun N-terminal kinase; MAP kinase, mitogen-activated protein kinase; OPG, osteoprotegerin.

Figure options

Prostaglandins act as autacoids in bone metabolism and play a pivotal role in bone cell functions [6]. Among them, it is generally recognized that PGE_1 is a potent bone-resorptive agent [6]. Currently, evidence is accumulating that prostaglandin is a mediator of bone remodeling [28]. Although OPG, which is synthesized and secreted from osteoblasts, plays an important role in suppression of osteoclastogenesis as a decoy receptor of RANKL [1], it seems likely that the negative regulation of OPG synthesis promotes proper bone remodeling required for maintaining the quality of bone. Adequate control of bone remodeling is necessary to maintain the bone mass and quality. In addition, proper osteoclastic bone resorption, an initial step of bone remodeling process, is essential to remove old fragile skeleton and its renewal. Taking our findings into account, it is possible that resveratrol as a physiological regulator affects the bone remodeling through the down-regulation of OPG production in osteoblasts. Further investigation is required to elucidate the detailed mechanism of resveratrol behind the OPG synthesis in osteoblasts.

In conclusion, our results strongly suggest that resveratrol suppresses PGE_1-stimulated OPG synthesis through inhibiting SAPK/JNK but not p38 MAP kinase in osteoblasts, and that the inhibitory effect of resveratrol is mediated at least in part through SIRT1 activation without up-regulating the expression.

Acknowledgements

We are very grateful to Yumiko Kurokawa for her skillful technical assistance. This investigation was supported in part by Grant-In-Aid for Scientific Research (19591042) from the Ministry of Education, Scienc e, Sports and Culture of Japan, the Foundation for Growth Science, the Research Funding for Longevity Sciences (23-9, 25-4) from National Center for Geriatrics and Gerontology (NCGG), Japan.

References

[1] P.A. Ross
Osteoclast biology and bone resorption
C.J Rosen (Ed.), Primer on the metabolic bone diseases of mineral metabolism (8th ed.), American Society for Bone and Mineral Research, Published by A John Wiley & Sons, Inc. (2013)

[2] G. Karsenty, E.F. Wagner
Reaching a genetic and molecular understanding of skeletal development
Dev Cell, 2 (2002), pp. 389–406

Article | PDF (398 K)

[3] A.M. Parfit
Targeted and nontargeted bone remodeling: relationship to basic multicellular unit organization and progression
Bone, 30 (2002), pp. 5–7

[4] W.S. Simonet, D.L. Lacey, C.R. Dunstan, et al.
Osteoprotegerin: a novel secreted protein involved in the regulation of bone density
Cell, 89 (1997), pp. 309–319

Article | PDF (3759 K)

[5] A. Mizuno, T. Kanno, M. Hoshi, et al.
Transgenic mice overexpressing soluble osteoclast differentiation factor (sODF) exhibit severe osteoporosis
J Bone Miner Metab, 20 (2002), pp. 337–344

[6] H. Hikiji, T. Takato, T. Shimizu, S. Ishii
The roles of prostanoids, leukotrienes, and platelet-activating factor in bone metabolism and disease
Prog Lipid Res, 47 (2008), pp. 107–126

Article | PDF (516 K)

[7] H. Tokuda, O. Kozawa, M. Miwa, T. Uematsu
p38 mitogen-activated protein (MAP) kinase but not p44/p42 MAP kinase is involved in prostaglandin E_1-induced vascular endothelial growth factor synthesis in osteoblasts
J Endocrinol, 170 (2001), pp. 629–638

[8] Y. Kanno, H. Tokuda, K. Nakajima, et al.
Involvement of SAPK/JNK in prostaglandin E_1-induced VEGF synthesis in osteoblast-like cells
Mol Cell Endocrinol, 220 (2004), pp. 89–95

Article | PDF (201 K)

[9] J. Jankun, S.H. Selman, R. Swiercz, E. Skrzypczak-Jankun
Why drinking green tea could prevent cancer
Nature, 387 (1997), p. 561

[10] J.B. Harbourne, C.A. Williams
Advances in flavonoid research since 1992
Phytochemistry, 55 (2000), pp. 481–504

[11] S.H. Koo, M. Montminy
In vino veritas: a tale of two sirt1s?
Cell, 127 (2006), pp. 1091–1093

Article | PDF (229 K)

[12] S. Renaud, M. de Lorgeril
Wine, alcohol, platelets, and the French paradox for coronary heart disease
Lancet, 339 (1992), pp. 1523–1526

Article | PDF (573 K)

[13] J.A. Baur, K.J. Pearson, N.L. Price, et al.
Resveratrol improves health and survival of mice on a high-calorie diet
Nature, 444 (2006), pp. 337–342

[14] H. Sudo, H. Kodama, Y. Amagai, S. Yamamoto, S. Kasai
In vivo differentiation and calcification in a new clonal osteogenic cell line derived from newborn mouse calvaria
J Cell Biol, 96 (1983), pp. 191–198

[15] O. Kozawa, H. Tokuda, M. Miwa, J. Kotoyori, Y. Oiso
Cross-talk regulation between cyclic AMP production and phosphoinositide hydrolysis induced by prostaglandin E_2 in osteoblast-like cells
Exp Cell Res, 198 (1992), pp. 130–134

Article | PDF (562 K)

[16] U.K. Laemmli
Cleavage of structural proteins during the assembly of the head of bacteriophage T4
Nature, 227 (1970), pp. 680–685

[17] K. Kato, H. Ito, K. Hasegawa, Y. Inaguma, O. Kozawa, T. Asano
Modulation of the stress-induced synthesis of hsp27 and αB-crystallin by cyclic AMP in C6 rat glioma cells
J Neurochem, 66 (1996), pp. 946–950

[18] J.C. Milne, P.D. Lambert, S. Schenk, et al.
Small molecule activators of SIRT1 as therapeutics for the treatment of type 2 diabetes

Nature, 450 (2007), pp. 712–716

[19] J.M. Kyriakis, J. Avruch
Mammalian mitogen-activated protein kinase signal transduction pathways activated by stress and inflammation
Physiol Rev, 81 (2001), pp. 807–869

[20] D.R. Alessi
PD 98059 is a specific inhibitor of the activation of mitogen-activated protein kinase kinase in vitro and in vivo
J Biol Chem, 270 (1995), pp. 27489–27494

[21] A. Cuenda, J. Rouse, Y.N. Doza, et al.
SB 203580 is a specific inhibitor of a MAP kinase homologue which is stimulated by cellular stresses and interleukin-1
FEBS Lett, 364 (1995), pp. 229–233

Article | PDF (699 K)

[22] B.L. Bennett, D.T. Sasaki, B.W. Murray, et al.
SP600125, an anthrapyrazolone inhibitor of Jun N-terminal kinase
Proc Natl Acad Sci U S A, 98 (2001), pp. 13681–13686

[23] G. Boily, X.H. He, B. Pearce, K. Jardine, M.W. McBurney
SirT1-null mice develop tumors at normal rates but are poorly protected by resveratrol
Oncogene, 28 (2009), pp. 2882–2893

[24] H.C. Chang, L. Guarente
SIRT1 and other sirtuins in metabolism
Trends Endocrinol Metab, 25 (2014), pp. 138–145

Article | PDF (550 K)

[25] G. Kuroyanagi, J. Mizutani, A. Kondo, et al.
Suppression by resveratrol of prostaglandin D_2-stimulated osteoprotegerin synthesis in osteoblasts
Prostaglandins Leukot Essent Fatty Acids, 91 (2014), pp. 73–80

Article | PDF (1130 K)

[26] G. Kuroyanagi, H. Tokuda, R. Matsushima-Nishiwaki, et al.
Resveratrol suppresses prostaglandin $F_{2\alpha}$-induced osteoprotegerin synthesis in osteoblasts: inhibition of the MAP kinase signaling
Arch Biochem Biophys, 542 (2014), pp. 39–45

Article | PDF (996 K)

[27] R.M. Breyer, C.K. Bagdassarian, S.A. Myers, M.D. Breyer
Prostanoid receptors: subtypes and signaling
Annu Rev Pharmacol Toxicol, 41 (2001), pp. 661–690

[28] D. Agas, L. Marchetti, M.M. Hurley, M.G. Sabbieti
Prostaglandin F2α: a bone remodeling mediator
J Cell Physiol, 228 (2013), pp. 25–29

Corresponding author at: Department of Clinical Laboratory, National Center for Geriatrics and Gerontology, Obu, Aichi 474-8511, Japan. Tel.: +81 562 46 2311; fax: +81 562 46 8396.

Resveratrol inhibits BMP-4-stimulated VEGF synthesis in osteoblasts: Suppression of S6 kinase

AKIRA KONDO[1,2], TAKANOBU OTSUKA[1], GEN KUROYANAGI[1,2], NAOHIRO YAMAMOTO[1,2], RIE MATSUSHIMA-NISHIWAKI[2], JUN MIZUTANI[1], OSAMU KOZAWA[2] and HARUHIKO TOKUDA[2,3]

[1]Department of Orthopedic Surgery, Nagoya City University Graduate School of Medical Sciences, Nagoya, Aichi 467-8601; [2]Department of Pharmacology, Gifu University Graduate School of Medicine, Gifu, Gifu 501-1194; [3]Department of Clinical Laboratory, National Center for Geriatrics and Gerontology, Obu, Aichi 474-8511, Japan

Received October 7, 2013; Accepted December 23, 2013

DOI: 10.3892/ijmm.2014.1626

Abstract. Resveratrol is well known as a natural polyphenol abundantly found in red wine. We previously reported that bone morphogenetic protein-4 (BMP-4) stimulates vascular endothelial growth factor (VEGF) synthesis via p70 S6 kinase in osteoblast-like MC3T3-E1 cells. In the present study, we investigated the effect of resveratrol on the BMP-4-stimulated VEGF synthesis in MC3T3-E1 cells. Resveratrol significantly suppressed BMP-4-stimulated release and expression levels of VEGF mRNA. SRT1720, an activator of SIRT1 with potencies greater than resveratrol, also reduced VEGF release and the mRNA levels. Both resveratrol and SRT1720 markedly attenuated the BMP-4-induced phosphorylation of p70 S6 kinase without affecting the BMP-4-induced phosphorylation of Smad1/5/8. These findings strongly suggest that resveratrol attenuates BMP-4-stimulated VEGF synthesis through suppression of the activation of p70 S6 kinase in osteoblasts, and that the inhibitory effect is mediated at least in part by SIRT1 activation.

Introduction

Bone metabolism is strictly regulated by osteoblasts and osteoclasts, which are responsible for bone formation and bone resorption, respectively (1). These functional cells are considered to affect one another via humoral factors as well as by direct cell-to-cell interaction. It has been firmly established that osteoblasts also play a crucial role in the regulation of bone resorption through receptor activator of nuclear factor-κB ligand (RANKL) expression in response to a variety of bone resorptive stimuli (2). The resorption of preexisting bone by osteoclasts and the formation of new bone by osteoblasts, bone remodeling, is a strictly coordinated process to maintain adequate bone mass. The disorder of bone remodeling causes metabolic bone diseases such as osteoporosis and fracture healing distress. In the process of bone remodeling, it is generally recognized that numerous humoral factors including cytokines and growth factors play pivotal roles (3).

Bone morphogenetic proteins (BMPs) are multifunctional cytokines and belong to the transforming growth factor-β (TGF-β) superfamily (4). It is well known that BMPs expressed in bone are essential for skeletal development and bone remodeling (5). The effects of BMPs on osteoblasts are exerted through Smad (Smad1/5/8)-dependent signaling and Smad-independent signaling such as the mitogen-activated protein (MAP) kinase family (4,6). Moreover, vascular endothelial growth factor (VEGF) is currently recognized to play critical roles in effective coupling of angiogenesis and osteogenesis (7). Among bone cells, the osteoblast lineage is considered as a major source of VEGF (7). In addition, the receptors for VEGF are expressed both on osteoblasts and osteoclasts (7). The production of VEGF by osteoblasts is reportedly modulated by a wide range of stimulations including hormonal, mechanical and environmental influences, suggesting that VEGF synthesis by osteoblasts plays a crucial role for the control of angiogenesis in bone via an autocrine and/or paracrine mechanism (7). We previously demonstrated that BMP-4 stimulates VEGF synthesis through activation of p70 S6 kinase in osteoblast-like MC3T3-E1 cells (8,9).

It has been firmly established that polyphenolic compounds in foods such as vegetables and fruits confer beneficial effects on human being. It has been reported that flavonoids, among the polyphenolic compounds, possess antioxidative, anti-inflammatory and anti-tumor effects (10,11). Resveratrol, a natural polyphenol found abundantly in the skins of red grapes and red wine, has recently received increased attention as a means to improve health and prolong life (12,13). In mammalian cells, the effects of resveratrol are recognized to be dependent upon SIRT1, known as a longevity gene, improving the function of cells and organs via activation of the nicotinamide adenine dinucleotide (NAD^+)-dependent deacetylase (14). Regarding the effects of resveratrol on bone, it has been shown that resveratrol promotes osteoblast differentiation (15,16). However,

Correspondence to: Dr Haruhiko Tokuda, Department of Clinical Laboratory, National Center for Geriatrics and Gerontology, Obu, Aichi 474-8511, Japan
E-mail: tokuda@ncgg.go.jp

Key words: resveratrol, bone morphogenetic protein-4, vascular endothelial growth factor, osteoblast

the exact mechanisms underlying the effects of resveratrol on bone metabolism have not yet been clarified.

In the present study, we investigated the effect of resveratrol on BMP-4-stimulated VEGF synthesis in osteoblast-like MC3T3-E1 cells and the related mechanisms. We demonstrated that resveratrol suppresses BMP-4-stimulated VEGF synthesis via inhibition of p70 S6 kinase in these cells.

Materials and methods

Materials. Resveratrol and SRT1720 were obtained from Calbiochem-Novabiochem Co. (La Jolla, CA, USA). BMP-4 and mouse VEGF enzyme-linked immunosorbent assay (ELISA) kits were obtained from R&D Systems, Inc. (Minneapolis, MN, USA). Phospho-specific Smad1/5/8 antibodies, phospho-specific p70 S6 kinase antibodies and p70 S6 kinase antibodies were obtained from Cell Signaling Technology, Inc. (Beverly, MA, USA). Glyceraldehyde-3-phosphate dehydrogenase (GAPDH) antibodies were obtained from Santa Cruz Biotechnology, Inc. (Santa Cruz, CA, USA). An ECL Western blotting detection system was obtained from GE Healthcare (Buckinghamshire, UK). TRIzol reagent was purchased from Invitrogen, Co. (Carlsbad, CA, USA). FastStart DNA Master SYBR-Green I was purchased from Roche Diagnostics (Mannheim, Germany). Omniscript Reverse Transcriptase kit was purchased from Qiagen, Inc. (Hilden, Germany). Other materials and chemicals were obtained from commercial sources. Resveratrol and SRT1720 were dissolved in dimethyl sulfoxide. The maximum concentration of dimethyl sulfoxide was 0.1%, which did not affect either the assay for VEGF or western blot analysis.

Cell culture. Cloned osteoblast-like MC3T3-E1 cells, which were derived from newborn mouse calvaria (17), were maintained as previously described (18). Briefly, the cells were cultured in α-minimum essential medium (α-MEM) containing 10% fetal calf serum (FCS) at 37˚C in a humidified atmosphere of 5% CO_2/95% air. The cells were seeded into 35-mm ($5x10^4$ cells/dish) or 90-mm ($2x10^5$ cells/dish) diameter dishes in α-MEM containing 10% FCS. After 5 days, the medium was replaced with α-MEM containing 0.3% FCS. The cells were used for experiments after 48 h.

Assay for VEGF. The cultured cells were pretreated with various doses of resveratrol, SRT1720 or vehicle for 60 min, and then stimulated with 70 ng/ml of BMP-4 or vehicle in 1 ml of α-MEM containing 0.3% FCS for the indicated periods. The conditioned medium was collected, and VEGF in the medium was then measured by mouse VEGF ELISA kits according to the manufacturer's protocol.

Real-time RT-PCR. The cultured cells were pretreated with 50 μM of resveratrol, 10 μM of SRT1720 or vehicle for 60 min, and then stimulated with 70 ng/ml of BMP-4 or vehicle in α-MEM containing 0.3% FCS for 24 h. Total RNA was isolated and transcribed into complementary DNA using TRIzol reagent and the Omniscript Reverse Transcriptase kit, respectively. Real-time RT-PCR was performed using a LightCycler system in capillaries and FastStart DNA Master SYBR-Green I provided with the kit. Sense and antisense primers for mouse VEGF or GAPDH mRNA were purchased from Takara Bio, Inc. (Tokyo, Japan) (primer set ID: MA039013). The amplified products were determined by melting curve analysis and agarose electrophoresis. VEGF mRNA levels were normalized with those of GAPDH mRNA.

Western blot analysis. The cultured cells were stimulated with BMP-4 for the indicated periods. When indicated, the cells were pretreated with resveratrol or SRT1720 for 60 min. The cells were washed twice with phosphate-buffered saline and then lysed, homogenized and sonicated in a lysis buffer containing 62.5 mM Tris/HCl, pH 6.8, 2% sodium dodecyl sulfate (SDS), 50 mM dithiothreitol and 10% glycerol. SDS-polyacrylamide gel electrophoresis (PAGE) was performed by the method described by Laemmli (19) on 10% polyacrylamide gels. Western blot analysis was performed as described previously (20) by using phospho-specific Smad1/5/8 antibodies, phospho-specific p70 S6 kinase antibodies, p70 S6 kinase antibodies or GAPDH antibodies, with peroxidase-labeled antibodies raised in goat against rabbit IgG being used as secondary antibodies. The peroxidase activity on the PVDF membrane was visualized on X-ray film by means of the ECL western blotting detection system.

Statistical analysis. The data were analyzed by ANOVA followed by Bonferroni method for multiple comparisons between pairs, and values of $P<0.05$ were considered to indicate statistically significant results. All data are presented as the mean ± standard error of the mean (SEM) of triplicate determinations from three independent cell preparations.

Results

Effect of resveratrol on BMP-4-stimulated VEGF release in MC3T3-E1 cells. We previously demonstrated that BMP-4 stimulates the synthesis of VEGF in osteoblast-like MC3T3-E1 cells (8). We first examined the effect of resveratrol on BMP-4-stimulated VEGF release. Resveratrol, which alone had little effect on VEGF levels, significantly suppressed BMP-4-stimulated VEGF release in MC3T3-E1 cells (Fig. 1). The inhibitory effect of resveratrol on VEGF synthesis was dose-dependent in the range between 10 and 70 μM (Fig. 2). Resveratrol (70 μM) caused an ~70% decrease in the BMP-4-mediated effect.

Effect of resveratrol on BMP-4-induced expression levels of VEGF mRNA in MC3T3-E1 cells. To investigate whether the suppressive effect of resveratrol on BMP-4-stimulated VEGF release is mediated through a transcriptional event, we next examined the effect of resveratrol on BMP-4-induced VEGF mRNA expression. Resveratrol significantly reduced the VEGF mRNA expression levels induced by BMP-4 (Fig. 3).

Effects of SRT1720 on the release of VEGF and the mRNA expression stimulated by BMP-4 in MC3T3-E1 cells. SRT1720 is also known as an activator of SIRT1 as well as resveratrol, and the potencies are estimated to be ~1,000-fold greater than resveratrol (21,22). Next, we investigated the effect of SRT1720 on BMP-4-stimulated VEGF synthesis in MC3T3-E1 cells. SRT1720, which alone had little effect on

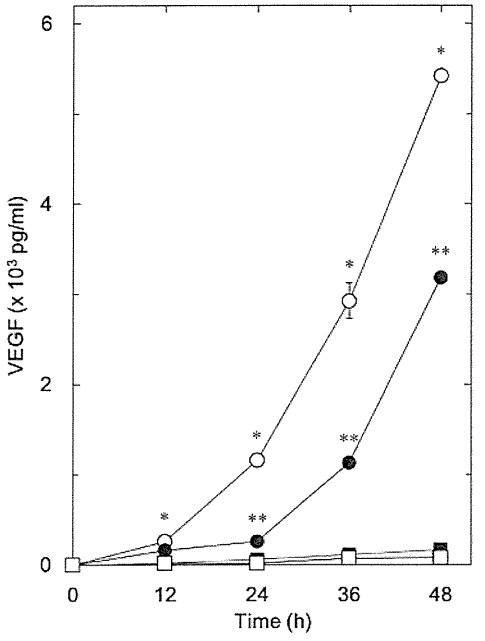

Figure 1. Effect of resveratrol on bone morphogenetic protein-4 (BMP-4)-stimulated vascular endothelial growth factor (VEGF) release in MC3T3-E1 cells. The cultured cells were pretreated with 50 μM of resveratrol (● and ■) or vehicle (○ and □) for 60 min, and then stimulated with 70 ng/ml of BMP-4 (● and ○) or vehicle (■ and □) for the indicated time periods. VEGF concentrations in the culture medium were determined by ELISA. Each value represents the mean ± standard error of the mean (SEM) of triplicate determinations from three independent cell preparations. *P<0.05, compared to the value of the control; **P<0.05, compared to the value in cells treated with BMP-4 alone.

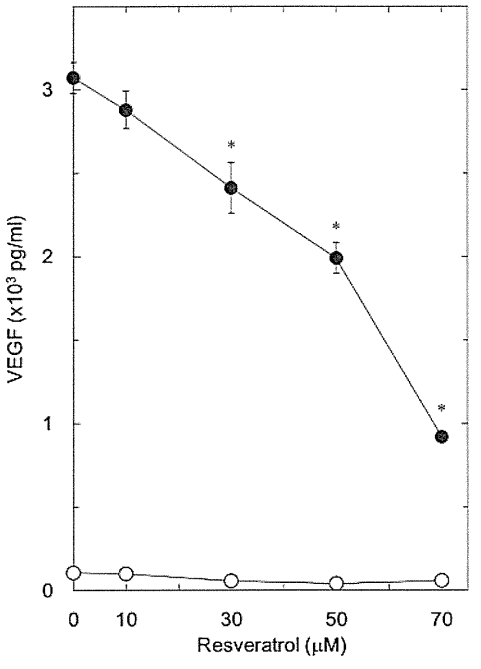

Figure 2. Dose-dependent effect of resveratrol on bone morphogenetic protein-4 (BMP-4)-stimulated vascular endothelial growth factor (VEGF) release in MC3T3-E1 cells. The cultured cells were pretreated with various doses of resveratrol for 60 min, and then stimulated with 70 ng/ml of BMP-4 (●) or vehicle (○) for 48 h, followed by measurement of VEGF in the respective media. VEGF concentrations in the culture medium were determined by ELISA. Each value represents the mean ± standard error of the mean (SEM) of triplicate determinations from three independent cell preparations. *P<0.05, compared to the value of the control.

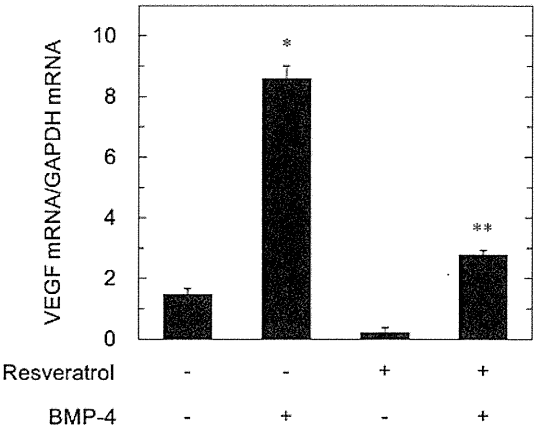

Figure 3. Effect of resveratrol on bone morphogenetic protein-4 (BMP-4)-induced expression levels of vascular endothelial growth factor (VEGF) mRNA in MC3T3-E1 cells. The cultured cells were pretreated with 50 μM of resveratrol or vehicle for 60 min, and then stimulated with 70 ng/ml of BMP-4 or vehicle for 24 h. The respective total RNA was then isolated and quantified by real-time RT-PCR. Each value represents the mean ± standard error of the mean (SEM) of triplicate determinations from three independent cell preparations. *P<0.05 compared to the value of the control; **P<0.05 compared to the value in cells treated with BMP-4 alone.

Table I. Effect of SRT1720 on BMP-4-stimulated VEGF release in MC3T3-E1 cells.

SRT1720	BMP-4	VEGF (pg/ml)
-	-	36.9±1.2
-	+	2577.0±202.1[a]
+	-	32.4±2.2
+	+	1124.4±46.1[b]

The cultured cells were pretreated with 10 μM of SRT1720 or vehicle for 60 min, and then stimulated with 70 ng/ml of BMP-4 or vehicle for 48 h, followed by measurement of VEGF in the respective media. Each value represents the mean ± SEM of triplicate determinations from three independent cell preparations. [a]P<0.05, compared to the value of the control. [b]P<0.05, compared to the value in cells treated with BMP-4 alone. BMP-4, bone morphogenetic protein-4; VEGF, vascular endothelial growth factor.

VEGF release, significantly suppressed the BMP-4-stimulated VEGF release (Table I). In addition, SRT1720, which alone did not affect the VEGF mRNA expression levels, significantly reduced the expression levels of VEGF mRNA induced by BMP-4 (Table II).

Effects of resveratrol or SRT1720 on the BMP-4-induced phosphorylation of Smad1/5/8 in MC3T3-E1 cells. It has been previously established that the effects of BMPs are exerted through the intracellular signaling of Smad proteins such as Smad1, Smad5 and Smad8 (4). In order to clarify whether the inhibitory effect of resveratrol on the BMP-4-stimulated VEGF synthesis is mediated by the modification of Smad1/5/8 activation in MC3T3-E1 cells, we examined the effect of resveratrol on the BMP-4-induced phosphorylation of Smad1/5/8. Resveratrol, which alone had little effect on the

Table II. Effect of SRT1720 on BMP-4-induced expression levels of VEGF mRNA in MC3T3-E1 cells.

SRT1720	BMP-4	VEGF mRNA/GAPDH mRNA
-	-	1.49±0.30
-	+	8.60±0.71[a]
+	-	1.51±0.26
+	+	5.94±0.12[b]

The cultured cells were pretreated with 10 μM of SRT1720 or vehicle for 60 min, and then stimulated with 70 ng/ml of BMP-4 or vehicle for 24 h. The respective total RNA was then isolated and quantified by real-time RT-PCR. Each value represents the mean ± SEM of triplicate determinations from three independent cell preparations. [a]P<0.05 compared to the value of the control. [**]P<0.05 compared to the value in cells treated with BMP-4 alone. BMP-4, bone morphogenetic protein-4; VEGF, vascular endothelial growth factor.

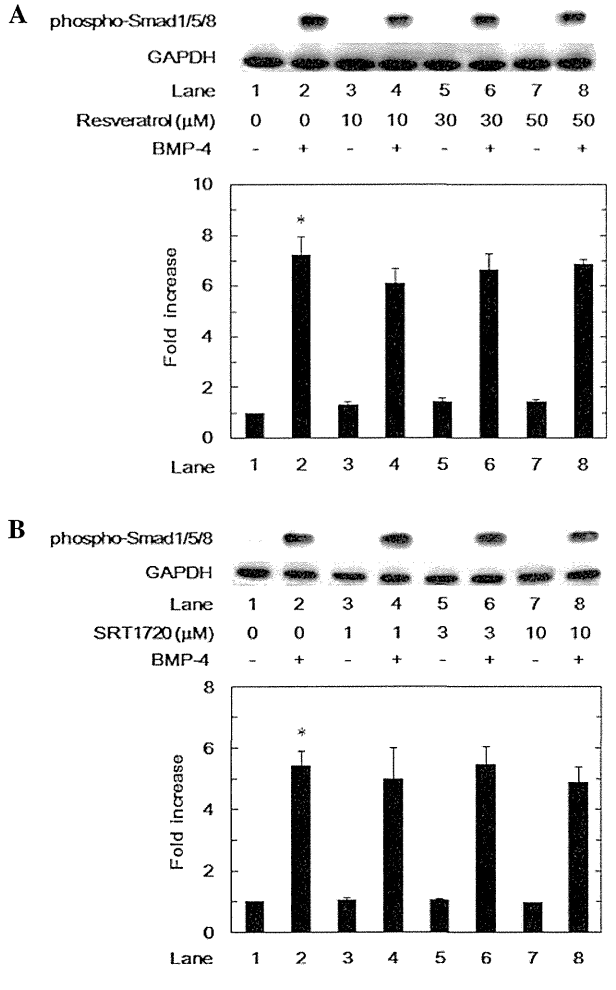

Figure 4. Effect of resveratrol or SRT1720 on bone morphogenetic protein-4 (BMP-4)-induced phosphorylation of Smad1/5/8 in MC3T3-E1 cells. The cultured cells were pretreated with various doses of resveratrol (A) or SRT1720 (B) for 60 min, and then stimulated with 30 ng/ml of BMP-4 or vehicle for 120 min. The cell extracts were then subjected to sodium dodecyl sulfate-polyacrylamide gel electrophoresis (SDS-PAGE) with subsequent western blot analysis with antibodies against phospho-specific Smad1/5/8 and GAPDH. The histogram shows the quantitative representation of the levels of BMP-4-induced phosphorylation obtained from a laser densitometric analysis of three independent experiments. Each value represents the mean ± standard error of the mean (SEM) of triplicate determinations. *P<0.05, compared to the value of the control.

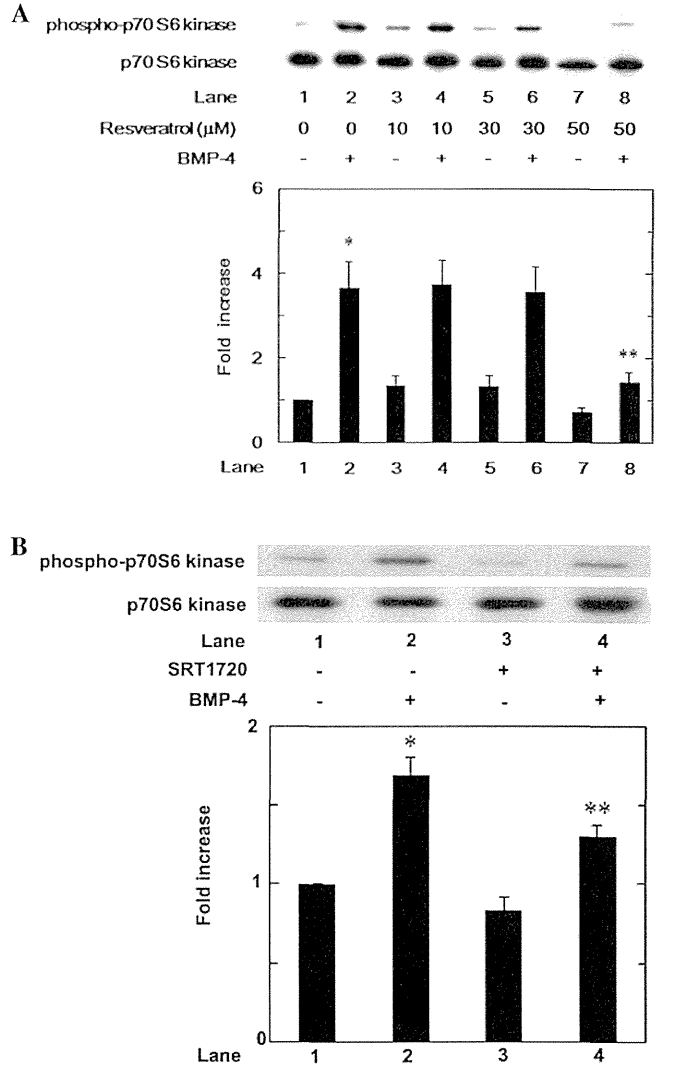

Figure 5. Effect of resveratrol or SRT1720 on bone morphogenetic protein-4 (BMP-4)-induced phosphorylation of p70 S6 kinase in MC3T3-E1 cells. The cultured cells were pretreated with various doses of resveratrol (A) or 10 μM of SRT1720 (B) for 60 min, and then stimulated with 30 ng/ml of BMP-4 or vehicle for 90 min. The cell extracts were then subjected to sodium dodecyl sulfate-polyacrylamide gel electrophoresis (SDS-PAGE) with subsequent western blot analysis with antibodies against phospho-specific p70 S6 kinase and p70 S6 kinase. The histogram shows the quantitative representation of the levels of BMP-4-induced phosphorylation obtained from a laser densitometric analysis of three independent experiments. Each value represents the mean ± standard error of the mean (SEM) of triplicate determinations. *P<0.05, compared to the value of the control; **P<0.05, compared to the value in the cells treated with BMP-4 alone.

phosphorylation levels of Smad1/5/8, failed to affect the levels induced by BMP-4 at a dose up to 50 μM (Fig. 4A). In addition, SRT1720 did not affect the Smad1/5/8 phosphorylation levels at a dose up to 10 μM (Fig. 4B).

Effects of resveratrol or SRT1720 on the BMP-4-induced phosphorylation of p70 S6 kinase in MC3T3-E1 cells. We previously demonstrated that BMP-4 stimulates VEGF synthesis through activation of p70 S6 kinase in osteoblast-like MC3T3-E1 cells (8). In order to elucidate whether the suppressive effect of resveratrol on BMP-4-stimulated VEGF synthesis is mediated by the modulation of p70 S6 kinase activation in